

Archetypes and Controls of Riverine Nutrient Export Across German Catchments

Pia Ebeling¹, Rohini Kumar², Michael Weber², Lukas Knoll³, Jan Fleckenstein⁴, and Andreas Musolff¹

¹UFZ - Helmholtz-Centre for Environmental Research

²UFZ-Helmholtz Centre for Environmental Research

³Justus Liebig University Giessen

⁴Helmholtz Center for Environmental Research - UFZ

November 22, 2022

Abstract

Elevated nutrient inputs and reduced riverine concentration variability challenge the health and functioning of aquatic ecosystems. To improve riverine water quality management, it is necessary to understand the underlying biogeochemical and physical processes and their interactions at catchment scale. We hypothesize that spatial heterogeneity of nutrient sources dominantly controls the variability of instream concentrations among different catchments. Therefore, we investigated controls of mean nitrate (NO), phosphate (PO), and total organic carbon (TOC) concentrations and concentration-discharge (C-Q) relationships from observations in 787 German catchments covering a wide range of physiographic and anthropogenic settings. Using partial least square regressions and random forests we linked water quality metrics to catchment characteristics. We found archetypal C-Q patterns with enrichment dominating NO and TOC, and dilution dominating PO export. Across the catchments, we found a positive but heteroscedastic relation between mean NO concentrations and agricultural land use. We argue that denitrification, particularly pronounced in sedimentary aquifers, buffers high inputs and causes a decline in concentration with depth resulting in chemodynamic, strongly positive C-Q patterns. Consequently, chemodynamic NO enrichment patterns could indicate effective subsurface denitrification. Mean PO concentrations were related to point sources though the low predictive power suggests effects of unaccounted processes. In contrast, diffuse inputs better explained the spatial differences in PO C-Q patterns. TOC levels were positively linked to the abundance of riparian wetlands as well as negatively to NO concentrations suggesting interacting processes. This study shows that vertical concentration heterogeneity mainly drives nutrient export dynamics, partially modified by interactions with other controls.

Hosted file

sinfo_20_06_09.docx available at <https://authorea.com/users/539239/articles/599860-archetypes-and-controls-of-riverine-nutrient-export-across-german-catchments>

Archetypes and Controls of Riverine Nutrient Export Across German Catchments

Pia Ebeling¹, Rohini Kumar², Michael Weber², Lukas Knoll³, Jan H. Fleckenstein^{1,4},
Andreas Musolff¹

¹Department of Hydrogeology, Helmholtz Centre for Environmental Research - UFZ, Leipzig, Germany.

²Department of Computational Hydrosystems, Helmholtz Centre for Environmental Research - UFZ, Leipzig, Germany.

³Institute for Landscape Ecology and Resources Management (ILR), Research Centre for BioSystems, Land Use and Nutrition (iFZ), Justus Liebig University Giessen, Giessen, Germany.

⁴Bayreuth Center of Ecology and Environmental Research (BayCEER), University of Bayreuth, Bayreuth, Germany.

Corresponding author: Pia Ebeling (pia.ebeling@ufz.de)

Key Points:

- Dynamics of riverine NO_3^- are controlled by vertical concentration heterogeneity resulting from subsurface reactivity
- Diffuse P sources exert an unexpectedly strong control on the spatial variability of PO_4^{3-} export patterns in contrast to point sources
- Riparian wetlands as source areas control mean TOC concentrations, yet export dynamics are not well explained by catchment characteristics

Abstract

Elevated nutrient inputs and reduced riverine concentration variability challenge the health and functioning of aquatic ecosystems. To improve riverine water quality management, it is necessary to understand the underlying biogeochemical and physical processes and their interactions at catchment scale. We hypothesize that spatial heterogeneity of nutrient sources dominantly controls the variability of instream concentrations among different catchments. Therefore, we investigated controls of mean nitrate (NO_3^-), phosphate (PO_4^{3-}), and total organic carbon (TOC) concentrations and concentration-discharge (C-Q) relationships from observations in 787 German catchments covering a wide range of physiographic and anthropogenic settings. Using partial least square regressions and random forests we linked water quality metrics to catchment characteristics. We found archetypal C-Q patterns with enrichment dominating NO_3^- and TOC, and dilution dominating PO_4^{3-} export. Across the catchments, we found a positive but heteroscedastic relation between mean NO_3^- concentrations and agricultural land use. We argue that denitrification, particularly pronounced in sedimentary aquifers, buffers high inputs and causes a decline in concentration with depth resulting in chemodynamic, strongly positive C-Q patterns. Consequently, chemodynamic NO_3^- enrichment patterns could indicate effective subsurface denitrification. Mean PO_4^{3-} concentrations were related to point sources though the low predictive power suggests effects of unaccounted processes. In contrast, diffuse inputs better explained the spatial differences in PO_4^{3-} C-Q patterns. TOC levels were positively linked to the abundance of riparian wetlands as well as negatively to NO_3^- concentrations suggesting interacting processes. This study shows that vertical concentration heterogeneity mainly drives nutrient export dynamics, partially modified by interactions with other controls.

Plain Language Summary

The major nutrients phosphorus, nitrogen and carbon, are main components of plants and all living organisms. Humans are altering the nutrient cycles especially to improve agricultural productivity. However, excess nutrients in surface waters have harmed many aquatic ecosystems through toxic algal blooms and loss of biodiversity. Low concentrations with a natural variability of concentrations are similarly important to those ecosystems but human interference with natural drivers is not yet fully understood. To unravel if natural or human controls dominate, we investigate nutrient concentrations and their variability over a wide range of different landscapes and conditions. The human impact is clearly visible for mean nitrate concentrations, while the subsurface properties seem to control the variability of riverine nitrate allowing to predict subsurface conditions from riverine nitrate dynamics. In the past phosphate inputs had usually been linked to wastewater, yet, we found the control of agricultural activities on concentration dynamics to be unexpectedly high. Organic carbon was associated mainly with natural sources related to riparian wetlands where interactions with other nutrients are possible. This understanding of dominant controls is important for adapting management strategies to ensure healthy aquatic ecosystems.

1 Introduction

Human activities put aquatic ecosystems under pressure by elevated nutrient inputs from fertilizer applications and wastewater sources. The health and functioning of stream ecosystems and eutrophication risk are strongly linked to levels and temporal variability of nutrient concentrations (Hunsaker & Johnson, 2017; Pascal et al., 2013; Withers & Jarvie, 2008). Moreover, the dynamics of nutrient concentrations in concert with discharge control nutrient

loads exported from catchments to downstream water bodies and finally to the oceans causing eutrophication in many estuaries of the world (Bricker et al., 1999; EEA, 2018). Adverse effects of eutrophication are hypoxia, toxic algal blooms, fish kills, loss of biodiversity, limitations for drinking water, and structural and functional changes in ecosystems (Le Moal et al., 2019; Smith, 2003; Smith et al., 1999). Therefore, eutrophication is one of the major global water quality concerns and understanding mobilization and retention processes of nutrients becomes crucial for a sustainable nutrient management.

Several national and European regulations have been adopted to reduce nutrient-related water quality problems. Initially, the focus was on reducing nutrient inputs related to point sources (BGBI.1, 1980; Copeland, 2016; ECC, 1991) but later regulations additionally addressed nonpoint-source pollution (Copeland, 2016; EEC, 1991, 2000). In the European Union, the Water Framework Directive (WFD, EEC, 2000) set water quality aims and guidelines including the reduction of diffuse pollution, e.g. from agricultural fields, and demanding a river basin and ecology-oriented perspective for water quality management. Still, many surface water bodies worldwide lack a good ecological status, with diffuse sources from agriculture being one of the main pressures (Damania et al., 2019; EEA, 2018; EPA, 2017).

Measures to improve the water quality are usually implemented and evaluated at catchment scale (e.g., Bouraoui & Grizzetti, 2011). Yet, catchments are complex and heterogeneous systems within which multiple biogeochemical and hydrological processes interact at different spatial and temporal scales (Bouwman et al., 2013; Clark et al., 2010), integrating into water quantity and quality responses observed at the catchment outlet (Bouraoui & Grizzetti, 2011). A considerable amount of nutrients can be retained or degraded in different compartments, such as soils, groundwater, riparian zones, and streams, altogether considered as successive filters, reducing loads transported downstream (Bouwman et al., 2013). The importance of processes on transported loads generally depends on the interplay between transport and reaction time scales (Musolff, Fleckenstein, et al., 2017; Oldham et al., 2013). Those may vary spatio-temporally creating “hot spots” and “hot moments” (McClain et al., 2003). Hierarchies and interactions among processes and different scales as well as differences among catchments are still not properly understood and upscaling of small-scale processes to the catchment scale remains a challenging task (e.g., Bol et al., 2018; Pinay et al., 2015).

Data-driven inductive analyses allow characterizing the observed integrated catchment responses and thereby inferring dominant processes, which operate within a catchment. By revealing linkages, top-down analyses provide approaches that allow for interpretation of drivers but cannot prove their causality, which can be further strengthened in combination with modeling and experimental work. Mean concentrations (C) indicate the general levels of nutrient stress, while concentration-discharge (C-Q) relationships classify solute export dynamics in terms of export regimes and patterns (Musolff et al., 2015), which reflects the underlying biogeochemical and hydrological processes. A chemostatic regime is defined as relatively low C variability compared to high discharge (Q) variability, while a chemodynamic regime defines a relatively high C to Q variability. Export patterns characterize the direction and strength of influence of Q on C. Enrichment or accretion patterns describe increasing C with increasing Q, while dilution describes decreasing C with increasing Q. Enrichment patterns emerge if additional sources get accessed with additional discharge generating areas (transport-limitation). On the other hand, dilution patterns prevail in supply-limited systems. When comparing C-Q relationships among different solutes and catchments, generalities and key controls of solute

export can be identified (Minaudo et al., 2019; Musolff et al., 2015; Zarnetske et al., 2018). Therefore, C-Q relationships have been widely applied to determine water quality and quantity functioning at different temporal (i.e. event, inter- and intra-annual, e.g. Dupas et al. (2016); Minaudo et al. (2019); Rose et al. (2018); Westphal et al. (2019)) and spatial scales (from hillslope and headwaters, e.g. Bishop et al. (2004); Herndon et al. (2015); Hunsaker and Johnson (2017), to numerous, large and nested catchments, e.g. Basu et al. (2010); Evans et al. (2014); Moatar et al. (2020)). Prevailing C-Q patterns depend on element properties (Minaudo et al., 2019; Moatar et al., 2017) while the encountered variability in export dynamics can partly be explained by catchment characteristics (e.g., Musolff et al., 2015). Variable end-member mixing and other time-variant controls of C can cause scatter in C-Q relationships (e.g., Burns et al., 2019), related to e.g. event hysteresis (e.g., Benettin et al., 2017; Tunaley et al., 2017), variable antecedent and seasonal conditions (e.g., Werner et al., 2019; Winterdahl et al., 2011) or changes in sources (e.g., Westphal et al., 2019).

To understand riverine nutrient export dynamics we require process understanding of the major elements of catchment scale transport – input, mobilization and retention. Nitrogen (N), phosphorus (P) and carbon are major macro nutrients but anthropogenic activities have altered their cycles and occurrence in water, including excess N and P in surface waters. Mean nitrate (NO_3) concentrations increase with higher shares of agricultural land (e.g., Evans et al., 2014; Hansen et al., 2018; Minaudo et al., 2019; Musolff et al., 2015), while phosphate (PO_4) concentrations have been mainly related to point sources (Minaudo et al., 2019; Westphal et al., 2019). With significant point source reductions, though, diffuse P emissions from agricultural soils become increasingly relevant (e.g., Bol et al., 2018; Le Moal et al., 2019; Schoumans et al., 2014). Elevated inputs could be counteracted by removal, e.g. by denitrification under anoxic conditions and availability of electron donors observed in wetlands (e.g., Hansen et al., 2018) and riparian zones (e.g., Lutz et al., 2020; Pinay et al., 2015; Rivett et al., 2008; Sabater et al., 2003), though local heterogeneities complicate the upscaling of removal capacities from site to catchment scale (Pinay et al., 2015). Moreover, denitrification can be small compared to temporary N retention related to assimilation in soil or stream compartments (Lutz et al., 2020). P retention and delivery to streams are closely linked to sorption in soils influenced by abiotic factors such as pH and redox conditions (Withers & Jarvie, 2008). During rewetting after warm periods or under anoxic conditions causing Fe hydroxide dissolution, riparian wetlands can act as a P source instead of as a sink for agricultural P (Dupas, Gruau, et al., 2015; Gu et al., 2017). For organic carbon, sources are linked to zones of organic matter accumulation, where biomass production exceeds removal via complete decomposition, e.g. in wetlands and peatlands (e.g., Clark et al., 2010). Therefore, riparian zones are important source areas (e.g., Clark et al., 2010; Kalbitz et al., 2000; Laudon et al., 2011; Musolff et al., 2018), where dissolved organic carbon (DOC) can also be consumed serving as electron donor in redox reactions e.g. denitrification. Riparian zones are usually hydrologically connected to the stream whereas more distant DOC source areas might not intersect discharge generating zones (Bishop et al., 2004). Riparian zones are thus potential hot spots of biogeochemical processes, including denitrification, DOC production and both P trapping and release, which are all linked to redox conditions and thus water table dynamics. After the delivery to the stream, instream processes, like redox reactions and uptake, can further remove, retain, transform or remobilize the nutrients before reaching the catchment outlet (Battin et al., 2008; Gomez-Velez et al., 2015).

Next to the sources, mobilization and transport mechanisms and reactivity together determine when and how dynamically constituents are exported. Generally, the interplay

between the solute source areas and hydrological connectivity has been found to control solute export dynamics (e.g., Herndon et al., 2015; Musolff, Fleckenstein, et al., 2017; Seibert et al., 2009; Thompson et al., 2011; Tunaley et al., 2017). If solute source areas are uniformly distributed in a catchment, a chemostatic regime establishes, typical for geogenic solutes (Thompson et al., 2011). Previous studies have found evidence that NO_3 often exhibits a chemostatic export regime in managed agricultural catchments (e.g., Basu et al., 2010; Basu et al., 2011; Dupas et al., 2016). This chemostatic regime is attributed to the build-up legacy of high N inputs in the past causing spatial homogenization of sources (Basu et al., 2010; Thompson et al., 2011), suggesting a significant anthropogenic impact on NO_3 export dynamics. Similarly, excess P inputs have led to P-legacies in soils and sediments (Jarvie et al., 2013; Schoumans et al., 2015; Sharpley et al., 2013). Legacy effects may hamper mitigation measures to reduce exported nutrient loads by dampening concentration responses and creating time lags (e.g., Bouraoui & Grizzetti, 2011; Howden et al., 2010; Meals et al., 2010; Van Meter & Basu, 2015; Wang et al., 2016). In contrast, chemodynamic regimes are related to heterogeneously distributed source areas and variable discharge generating zones (e.g., Musolff, Fleckenstein, et al., 2017; Zhi et al., 2019). Source heterogeneity can be linked, for example, to distinct production zones and resulting vertical soil distribution profiles (Seibert et al., 2009) and landscape patterns (Dupas, Gascuel-Odoux, et al., 2015; Herndon et al., 2015) as shown for DOC and to heterogeneous land use patterns and connected inputs such as fertilizers (Musolff, Fleckenstein, et al., 2017). Chemodynamic exports can also result from reactions along flow paths affecting longer travel times more than shorter ones leading to enrichment patterns for removal (Musolff, Fleckenstein, et al., 2017) and dilution for production or accumulation processes (Ameli et al., 2017; Musolff, Fleckenstein, et al., 2017). Moreover, transient processes can cause temporal variations in source zones, e.g. long-term input changes from fertilizer applications (Ehrhardt et al., 2019) or temporally variable production and accumulation in drying and wetting cycles (Gu et al., 2017). In summary, chemodynamic regimes signal variable combinations of discharge generating zones with different solute source strengths, travel times and reactivity along the flow paths within a catchment.

The anthropogenic impact on nutrient cycles and their consequence for concentration levels in streams (e.g., Gruber & Galloway, 2008; Hansen et al., 2018; Howden et al., 2010) as well as for nutrient export regimes has been discussed in several studies. However, only few studies to date have used a large number of catchments and various solutes to draw more general conclusions which requires a large sample size (Gupta et al., 2014). Thus it remains uncertain how general and wide-spread the anthropogenic impact and resulting homogeneity or heterogeneity of sources is over a wide range of landscapes compared to natural controls, heterogeneity and reactivity, and how persistent the effect of anthropogenic-induced chemostatic export is (Ehrhardt et al., 2019; Van Meter & Basu, 2017). Therefore, we seek to understand (1) what drives nutrient concentration levels and dynamics across a large variety of catchments and (2) how anthropogenic impacts such as nutrient inputs interact with natural factors such as the hydroclimate, topography, and subsurface conditions. Our exploratory analysis is guided by the hypothesis that spatial heterogeneity of diffuse sources is the major control of the variability of riverine nutrient concentrations.

To this end, we use mean C and C-Q relationships of $\text{NO}_3\text{-N}$, $\text{PO}_4\text{-P}$ and total organic carbon (TOC) to investigate and classify riverine nutrient dynamics in 787 independent catchments in Germany covering a wide range of ecoregions and large gradients in physical and hydroclimatic properties. We assess the predictive power of anthropogenic and natural catchment

properties to infer dominant controls and hypothesize about underlying processes by linking the descriptors to C-Q export metrics with partial least square regression (PLSR) and random forest (RF) models. Potential predictors include topography, land cover, geology, hydroclimate, diffuse and point sources and proxies for spatial source heterogeneity. This approach allows addressing the generality of patterns, testing existing hypothesis on a large number of catchments and discussing hierarchies of natural and anthropogenic controls of export metrics. Knowledge on drivers of nutrient export potentially serves to improve nutrient export models at catchment scale and develop management tools.

2 Materials and Methods

2.1. Water Quality and Quantity Data Set

Water quality data from river stations across Germany were gathered from the German Federal state environmental authorities (Musolff, 2020; Musolff et al., 2020). The authorities regularly monitor the surface water quality in the context of the WFD (EEC, 2000) taking grab samples with a biweekly to seasonal frequency. Here, we focussed on the major nutrients: nitrate-N concentrations as the dominant form of dissolved N (NO_3^- -N), the biologically available dissolved orthophosphate-phosphorus (PO_4^{3-} -P) and total organic carbon concentrations (TOC). For carbon, we used TOC instead of DOC samples because of better data availability and a strong correlation with a regression slope of about 0.87 between mean DOC and TOC concentrations (see Figure S1), and DOC representing about $81.3 (\pm 7.9) \%$ of TOC on average. For water quantity, daily mean discharge time series at the water quality locations were partly provided together with the quality data (Musolff, 2020; Musolff et al., 2020).

Out of the initial pool of 6000 sites, water quality time series were selected based on the following criteria concerning the quality and availability of concentration data and spatial data:

1) Data availability of at least three years in target period from 2000 to 2015. This time period excludes major changes of the 1990s when major improvements of wastewater treatment were put into place (Westphal et al., 2019).

2) Minimum of 70 concentration samples after outlier removal. As the large number of sites demanded a cost-effective method, only extreme outliers likely to be typographical errors were removed (following Oelsner et al., 2017). We defined outliers as concentrations $> \text{mean } C + 4 \times \text{standard deviation in logarithmic space}$ (confidence level $> 99.99 \%$ assuming lognormal distribution of concentrations) and as $\text{PO}_4\text{-P concentrations} > 100 \text{ mg l}^{-1}$, and TOC concentrations $> 1000 \text{ mg l}^{-1}$ in terms of absolute values.

3) Seasonal coverage of the concentration data, i.e. the samples within any of the four seasons (starting in October, November and December) constitutes at least 10% of the samples on average. This includes stations with data systematically missing in one month.

4) Left censored data of the concentration time series (values below the detection limit) must be less than 50% of the samples.

5) Catchment area must be delineable from topography, i.e. we excluded stations with apparent, major deviations between location of real river network and topography-based basin area. The catchments were delineated based on flow accumulation derived from a digital elevation model (DEM, EEA, 2013) of 25 m resolution resampled to 100 m and the river network from the CCM River and Catchment Database (version 2.1 (CCM2)(De Jager & Vogt,

2007)) with some manual adaptations of river segments which drastically improve the match between catchments and the real river network.

6) Independence of catchments, which was defined as nested catchments sharing less than 20% of their catchment area with any upstream station.

7) Station must not be directly located at the outlet of a reservoir or lake, because the water quality is expected to be mainly a result of lake dynamics, thus masking the catchment processes.

8) Data availability of catchment characteristics. This leads to the criterion that a minimum of 70% of the catchment area must fall within the borders of Germany, as some of the geodata were limited to Germany, such as N-surplus and point sources (see Section 2.3).

Applying the above criteria resulted in a set of 787 catchments with 759 NO₃-N, 695 PO₄-P, and 722 TOC time series. Out of those catchments, at 278 sites observed daily discharge data were available. Altogether, the analysed data base consists of a total of 110,603 concentration samples for combinations of dates and locations with an average between 135 (TOC) and 142 (NO₃-N) samples per site (from 2000 to 2015).

2.2. Metrics of Water Quality Dynamics

We used mean concentrations and metrics of the C-Q relationships to characterize the nutrient concentration levels and dynamics in the different catchments. Before calculating basic statistics at each station, i.e. mean concentrations and the standard deviation, we replaced the concentration values falling below the detection limit (left censored data) with half of the detection limit (see e.g., Hunsaker & Johnson, 2017; Underwood et al., 2017). Slope b of the linear relation between logarithmic concentration (C) and discharge (Q) following: $\log(C) = \log(a) + b \cdot \log(Q)$ (equals power law relationship $C = a \cdot Q^b$) (Godsey et al., 2009) was calculated for all stations. Slope b characterizes the export pattern of a solute or particulates: $b > 0$ indicates an enrichment or accretion pattern, $b < 0$ a dilution pattern, while $b \approx 0$ describes a non-significant, neutral C-Q pattern (Musolff, Fleckenstein, et al., 2017). Note that we consider a distinction between the export patterns based on the significant difference of the slope b from zero (t-test, 95% significance level) more appropriate than fixed, predefined range of slope b that have also been used (Herndon et al., 2015; Zimmer et al., 2019). Further note that slope b was determined up to censoring degrees of 20% by excluding the censored values from the regression assuming that no major part of the C-Q relationship will be missed by the data.

Additionally, we used the ratio of the coefficients of variation of concentration and discharge CV_C/CV_Q to characterize export regimes (Thompson et al., 2011). If CV_C/CV_Q is small (< 0.5), the export regime is chemostatic (i.e. C variations are small compared to variations in Q), while high values CV_C/CV_Q indicate a chemodynamic (i.e. C variations are large compared to variations in Q) export regime (Musolff et al., 2015). The combination of both statistics: slope b and CV_C/CV_Q allows distinguishing combinations of chemostatic and chemodynamic regimes within the different export patterns. This distinction is especially important for non-significant C-Q relationships, which can still demonstrate a chemodynamic export with C variability related to other factors than Q .

Based on the combination of export patterns and regimes, the studied catchments were categorized into six distinct export classes (see Supplementary Figure S2). Differences in mean concentrations between the export patterns and regimes were tested for significance ($\alpha=0.05$)

using a Kruskal-Wallis rank sum test. In case of significant differences between the C-Q patterns, the Wilcoxon rank sum test was used for pairwise comparisons to identify which patterns differ.

2.3. Catchment Characteristics

The 278 C-Q catchments with available discharge data cover an area of 43.7% of Germany, while the 787 C catchments cover 65.6%. Catchment sizes vary from 1.9 to 77099.2 km² (4.4 to 23162.7 km² for C-Q catchments), with 50% of the catchments < 97.1 km² (< 235.6 km²) and 95% < 1257.4 km² (< 2540.0 km²). The catchments intersect all 10 hydrogeological regions in Germany (BGR & SGD, 2015) and span a wide range of topographical, hydroclimatic, lithological and soil properties with varying anthropogenic presence. A summary of calculated characteristics is given in Table 1 and represented distributions of selected catchment characteristics, matching mean conditions in Germany, are shown in Figure 1. The selection of characteristics to consider was inspired by several previous studies (e.g., Botter et al., 2013; Dupas, Delmas, et al., 2015; Moatar et al., 2017; Musolff et al., 2018; Musolff et al., 2015; Onderka et al., 2012) and limited by availability over the large scale.

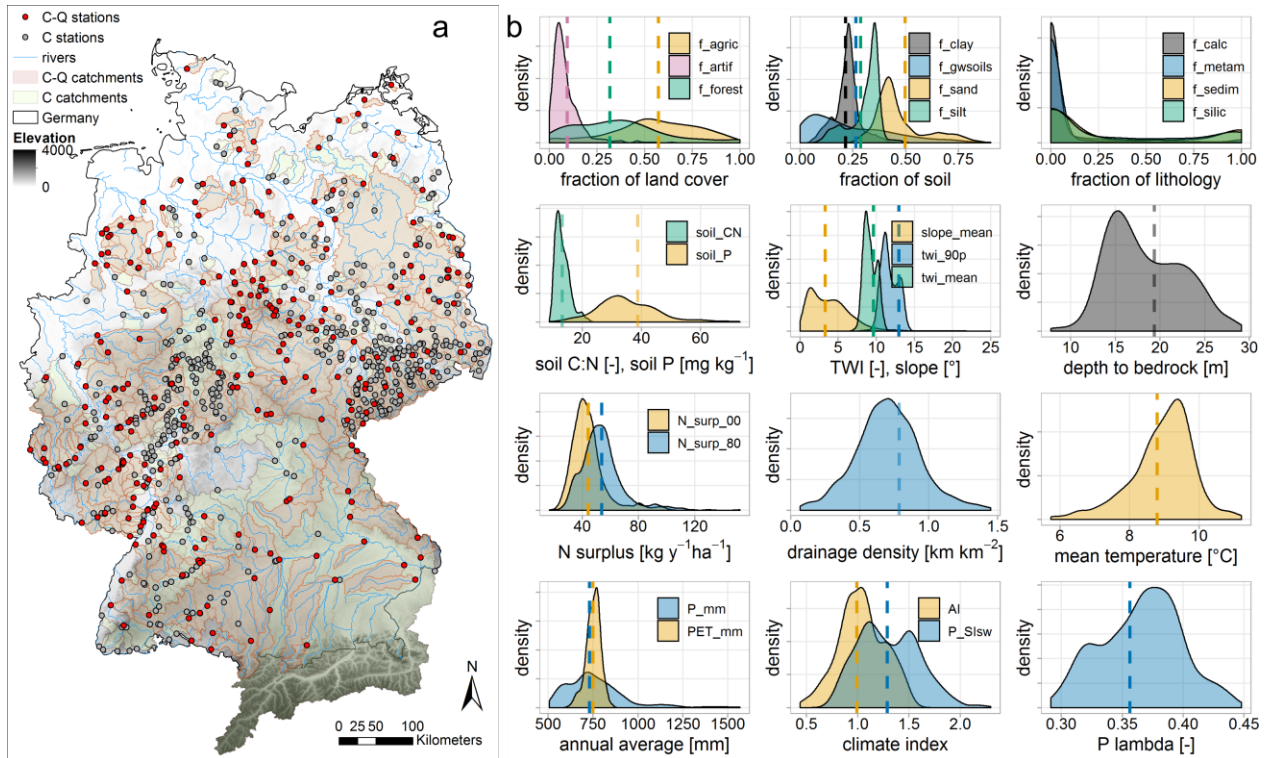


Figure 1. The study area with stations of concentration (C) and additional discharge (C-Q) data and corresponding catchments overlaying elevation (a) and distributions of selected catchment characteristics represented by the C catchments (b). TWI – topographic wetness index, P_{mm} – precipitation, PET_{mm} – potential evapotranspiration, AI – aridity index. For further abbreviations and explanations of the parameters refer to Table 1. Vertical dashed lines mark corresponding average values for Germany.

Table 1. Catchment Descriptors Used in the Analysis, Associated Methods and Data Sources

Category	Variable	Unit	Description and method	Data source
----------	----------	------	------------------------	-------------

Topography	area	km ²	Catchment area	
	dem_mean	mamsl	Mean elevation of catchment, from DEM rescaled from 25 to 100 m resolution using average	EEA (2013)
	slope_mean	°	Mean topographic slope of catchment, from DEM	EEA (2013)
	twi_mean	-	Mean topographic wetness index (TWI, Beven & Kirkby, 1979)	EEA (2013)
	twi_90p	-	90 th percentile of the TWI as a proxy for riparian wetlands (following Musolff et al., 2018)	EEA (2013)
	drain_dens	km ⁻¹	Average drainage density of the catchment. Gridded drainage density is provided as the length of surface waters (rivers and lakes) per area from a 75km ² circular area around each cell center.	BMU (2000)
Land cover	f_urban	-	Fraction of artificial land cover	CLC (2016)
	f_agric	-	Fraction of agricultural land cover	CLC (2016)
	f_forest	-	Fraction of forested land cover	CLC (2016)
	f_wetland	-	Fraction of wetland cover	CLC (2016)
	f_water	-	Fraction of surface water cover	CLC (2016)
	p_dens	persons km ⁻²	Mean population density	CIESIN (2017)
Nutrient sources	N_surp_00	kg N ha ⁻¹ y ⁻¹	Mean nitrogen surplus per catchment during sampling period (2000-2015) including N surplus on agricultural land and atmospheric deposition on non-agricultural areas	Bach et al. (2016); Häußermann et al. (2019)
	N_surp_80	kg N ha ⁻¹ y ⁻¹	Mean N surplus per catchment before and during sampling period (1980-2015) to consider historic (legacy) inputs	Bach et al. (2016); Häußermann et al. (2019)
	N_WW	kg N ha ⁻¹ y ⁻¹	Sum of N input from point sources including waste water treatment plants (WWTP) > 2000 person equivalents from the database of the European Environment Agency covering areas beyond Germany and data collected from 13 Federal German States covering smaller WWTP within Germany	Büttner (2020a, 2020b)
	P_WW	kg P ha ⁻¹ y ⁻¹	Sum of P input from WWTP analogous to N_WW	Büttner (2020a, 2020b)
	het_h	-	Slope of relative frequency of source areas in classes of flow distances to stream as a proxy for horizontal source heterogeneity (see in text Section 2.3)	Source areas based on Pflugmacher et al. (2018)
	sdist_mean	m	Mean lateral flow distance of source areas to stream (see in text Section 2.3)	Source areas based on Pflugmacher et al. (2018)
	het_v	-	Mean ratio between potential seepage and groundwater NO ₃ -N concentrations as proxy for vertical concentration heterogeneity (see in text Section 2.3)	Knoll et al. (2020)
Lithology and soils	f_calc	-	Fraction of calcareous rocks	BGR & UNESCO (eds.) (2014)
	f_calc_sed	-	Fraction of calcareous rocks and sediments	BGR & UNESCO (eds.) (2014)
	f_magma	-	Fraction of magmatic rocks	BGR & UNESCO (eds.) (2014)
	f_metam	-	Fraction of metamorphic rocks	BGR & UNESCO (eds.) (2014)
	f_sedim	-	Fraction of sedimentary aquifer	BGR & UNESCO (eds.) (2014)
	f_silic	-	Fraction of siliciclastic rocks	BGR & UNESCO (eds.) (2014)
	f_sili_sed	-	Fraction of siliciclastic rocks and sediments	BGR & UNESCO (eds.) (2014)
	dtb	cm	Median depth to bedrock in the catchment	Shangguan et al. (2017)
	f_gwsoils	-	Fraction of water-impacted soils in the catchment (from soil map 1:250,000), including stagnosols, semi-terrestrial, semi-subhydric, subhydric and moor soils	BGR (2018)
	f_sand	-	Mean fraction of sand in soil horizons of the top 100 cm	FAO/IIASA/ISRIC/ISSC AS/JRC (2012)
	f_silt	-	Mean fraction of silt in soil horizons of the top 100 cm	
	f_clay	-	Mean fraction of clay in soil horizons of the top 100 cm	
	water_root	mm	Mean available water content in the root zone from pedo-	Livneh et al. (2015); Samaniego et al. (2010);

			transfer functions	Zink et al. (2017)
theta_S	-		Mean porosity in catchment from pedo-transfer functions	Livneh et al. (2015); Samaniego et al. (2010); Zink et al. (2017)
soil_N	g kg ⁻¹		Mean top soil N in catchment	Ballabio et al. (2019)
soil_P	mg kg ⁻¹		Mean top soil P in catchment	Ballabio et al. (2019)
soil_CN	-		Mean top soil C/N ratio in catchment	Ballabio et al. (2019)
Climate	P_mm	mm	Mean annual precipitation (period 1986-2015 used for all climatic variables)	Cornes et al. (2018)
	P_Slsw	-	Seasonality of precipitation as the ratio between mean summer (Jun-Aug) and winter (Dec-Feb) precipitation	Cornes et al. (2018)
	P_lambda	-	Mean precipitation frequency λ as used by Botter et al. (2013)	Cornes et al. (2018)
	PET_mm	mm	Mean potential evapotranspiration	Cornes et al. (2018)
	AI	-	Aridity index as $AI = PET_mm / P_mm$	Cornes et al. (2018)
	T_mean	°C	Mean annual temperature	Cornes et al. (2018)

Next to climatic characteristics available for all catchments, hydrological characteristics were calculated for a smaller subset of catchments where daily discharge measurements were available (n=186). The hydrological variables include mean discharge, specific discharge, runoff coefficient, seasonal ratio, base flow index (BFI, WMO, 2008) and flashiness index based on flow percentiles following Jordan et al. (2005). More details on the hydrological variables and results are presented in the supporting information (Table S3 and S9-11).

To test our guiding hypothesis over a wide range of catchments, we parameterize source heterogeneity from landscape characteristics. Inspired by Musolff, Fleckenstein, et al. (2017), who found “structured heterogeneity” - defined as nonlinear correlation between source concentration and travel time - dominantly shape C-Q relationships, we aim at connecting discharge generating zones (implicitly related to travel times and water ages) with source distributions. Thereby, we focus on parameterizing the prevailing structured heterogeneity in each catchment as opposed to random variability and divide it into a horizontal and a vertical parameterization component as shown in Figure 2.

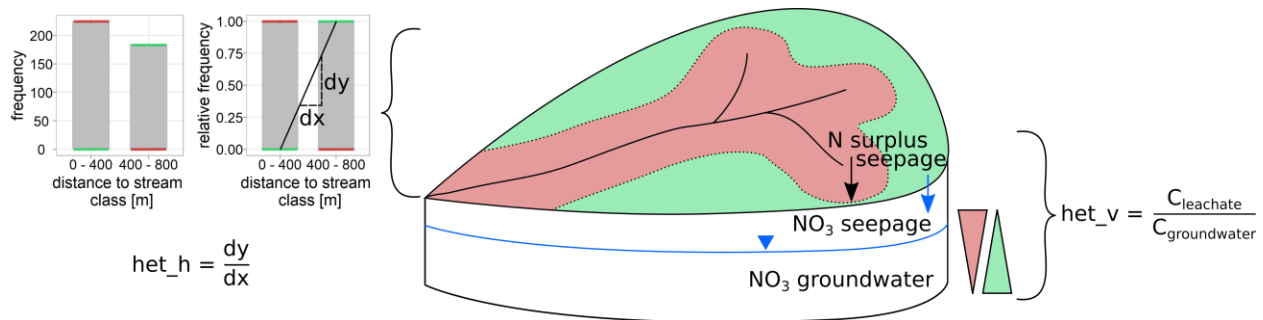


Figure 2. Conceptualized parameterization for two different scenarios of horizontal source (red area - sources close to stream, green area - sources relatively far from stream) and vertical concentration heterogeneity (red – top-loaded concentration profile, green – bottom-loaded). If $het_h < 0$ it represents systems with sources relatively close to the stream, $het_h = 0$ homogeneously distributed, $het_h > 0$ relatively far from the stream. If $het_v < 1$ it represents a bottom-loaded, $het_v = 1$ homogeneous and $het_v > 1$ a top-loaded concentration profile. For horizontal source heterogeneity only two distance classes are shown for simplicity while more classes are used for the real catchments.

For the horizontal source heterogeneity component of diffuse sources of $\text{NO}_3\text{-N}$ and $\text{PO}_4\text{-P}$ we assumed horizontal flow distances from the solute source to the stream network to link to flow paths and thus travel times. Source areas were defined as seasonal, perennial cropland and grassland land cover classes using a highly resolved land use map (Pflugmacher et al., 2018) representing diffuse anthropogenic nutrient sources. We computed horizontal flow distances along the topographic flow direction towards the stream using the ESRI ArcGIS (version 10.6). The stream grid was derived from the EU-wide EU-Hydro river network (EEA, 2016). According to the flow distance grid we resampled the land cover map with a 30 m resolution to 100 m using the majority method. For each catchment, we determined the mean source area distance to stream (sdist_mean) and the fraction of source area within classes of flow distances of 400 m each. Subsequently, we fitted a linear regression to the class values of the histogram weighed by the corresponding class frequencies within the catchment. If the slope of this regression is positive ($\text{het_h} > 0$), source areas tend to be located further from the stream, while if it is negative ($\text{het_h} < 0$), sources tend to be closer, and if $\text{het_h} = 0$, sources are homogeneously distributed. Thus the slope is a proxy for horizontal source heterogeneity comparable to the parameter γ in Musolff, Fleckenstein, et al. (2017). As the EU-Hydro river network partly deviates from delineated catchments and contains different degrees of details, 78 C and 38 C-Q catchments, especially small ones, contain implausible distance distributions. Therefore, catchments without intersection with any river segment or a maximum flow distance above 15 km were assigned as missing data. While these missing values lower the sample size, the related variables (het_h and sdist_mean) did not rank among the dominant predictors (as shown in the Results section) and therefore had been excluded from the main analysis results presented in Section 3.4. For the sake of completeness, analysis results corresponding to het_h and sdist_mean are presented in the supporting information (Table S4-5).

Similar to the horizontal source heterogeneity, we parameterized the vertical concentration heterogeneity as concentration gradients over depth. We again assume a link between flow paths over depth and travel times. For each catchment, we calculated the mean of the ratio between the potential seepage NO_3 concentrations and groundwater NO_3 concentrations as shown in Figure 2, resembling the parameter C_{ratio} used in Zhi et al. (2019). We used the groundwater NO_3 and potential seepage concentrations across Germany presented by Knoll et al. (2020). They estimated groundwater NO_3 concentrations with 1km resolution using a random forest model based on mean observed groundwater concentrations over the years 2009-2018 and spatial predictors, as previously introduced by Knoll et al. (2019). The potential seepage NO_3 concentrations (Knoll et al., 2020) were calculated as a ratio of N surplus (Bach et al., 2016; Häußermann et al., 2019) and the seepage rate (BGR, 2003). Due to data availability, vertical heterogeneity parameterization was calculated for NO_3 only but used as a descriptor for all nutrients.

2.4. Linking Water Quality Metrics to Descriptors

We applied Partial Least Squares Regressions (PLSR, Wold et al., 2001) in combination with the Variable Influence of Projection (VIP, Wold et al., 2001) and Random Forests (RF, Breiman, 2001) to identify controls for differences in mean concentrations, export patterns and regimes of $\text{NO}_3\text{-N}$, $\text{PO}_4\text{-P}$ and TOC among the studied catchments. Both models provide variable importance measures and can handle co-linearity between the descriptors as required in this study (see Figure S3 and Section 3.4) to link continuous variables, while PLSR is a linear and RF a non-linear method. Both models have been applied in water quality studies, e.g. PLSR for

investigating solute export and their predictors (Musolff et al., 2015; Onderka et al., 2012; Wallin et al., 2015) and RF for estimating spatial distributions of groundwater NO_3 concentrations (Knoll et al., 2019; Ouedraogo et al., 2019; Rodriguez-Galiano et al., 2014) and artificial drainage systems (Møller et al., 2018). Here, we combine the two different approaches as a model ensemble to improve the interpretability in terms of generalities in the identified dominant predictors and thus face uncertainties related with data-driven analysis approaches, as proposed e.g. by Schmidt et al. (2020).

One PLSR and one RF model per response variable was set up using the catchment characteristics listed in Table 1 as descriptors for the complete set of catchments (excluding *sdist_mean* and *het_h*). Besides, models including either *sdist_mean* and *het_h* or hydrological descriptors were run for a small number of catchments due to missing values and presented in the supporting information (Table S4-5). Nutrient-specific point sources were considered only for the corresponding nutrient (i.e. either $\text{NO}_3\text{-N}$ or $\text{PO}_4\text{-P}$). For diffuse sources, only N surplus data were available and used as a descriptor for all nutrients because of expected correlations to P surplus (Minaudo et al., 2019) and other possible interactions between the nutrient-cycles (Gruber & Galloway, 2008). N surplus was thus considered as a proxy for agricultural, diffuse P inputs together with the topsoil P content. All data were standardized to unit variance and zero mean to give the variables the same prior importance and enhance the model stability (Wold et al., 2001). Furthermore, we used simple and multiple linear regression for selected descriptors complementing the information on variable importance and the variance explained by the complete PLSR and RF models to explore and explain relationships between descriptors and export metrics.

To assess the model performances and to tune the number of components in PLSR, we conducted a 3 times repeated 10-fold cross-validation (for model tuning settings see Table S1). For RF, the number of trees was set to 500 and the number of randomly sampled descriptors used at each split was fixed to 11 based on an exemplary tuning which showed similar performances for similar values. The variable importance of each predictor in the RF models was assessed based on the mean increase of accuracy based on “out-of-bag” (OOB) samples from the training process. The analysis was conducted with the *caret* package (version 6.0-84) in R (version 3.5.0) and partial dependence plots created with the *pdp* package in R (version 0.7.0.).

3 Results

3.1. Classification of C-Q Metrics and Mean Concentrations

Basic statistics of the catchments' mean concentrations and C-Q metrics are given in Table 2. Overall, the studied catchments showed average mean concentrations of $4.06 \text{ mg l}^{-1} \text{ NO}_3\text{-N}$, $0.12 \text{ mg l}^{-1} \text{ PO}_4\text{-P}$, and $5.88 \text{ mg l}^{-1} \text{ TOC}$. The average coefficient of variation of concentration CV_C varied between 0.38 for $\text{NO}_3\text{-N}$, 0.41 for TOC, and 0.68 for $\text{PO}_4\text{-P}$. In general, C-Q metrics covered all types of patterns and regimes with mean slope $b > 0$ and mean $\text{CV}_C/\text{CV}_Q < 0.5$ for $\text{NO}_3\text{-N}$ and TOC and mean slopes $b < 0$ and mean $\text{CV}_C/\text{CV}_Q > 0.5$ for $\text{PO}_4\text{-P}$, while for all nutrients standard deviations of b were larger than absolute mean b . The C-Q power-law regressions showed nearly similar model performances for the three nutrients with mean $R^2 = 0.27 \pm 0.24$ for $\text{NO}_3\text{-N}$ slightly higher than $\text{PO}_4\text{-P}$ ($R^2 = 0.21 \pm 0.19$) and TOC ($R^2 = 0.19$

± 0.20). The highest individual R^2 across the study catchments was found for TOC (maximum $R^2=0.85$), closely followed by $\text{NO}_3\text{-N}$ (maximum $R^2=0.84$) and $\text{PO}_4\text{-P}$ (maximum $R^2=0.72$).

Table 2. Summary Statistics of the Calculated Metrics of Concentration (C) and Concentration-Discharge (C-Q) Relationships.

	Concentration				C-Q relationships			
	n C-catchments with <50% censored data	Mean [mg l ⁻¹]	Median [mg l ⁻¹]	CV _C	n C-Q-catchments with <50% (<20%) censored data	CV _C /CV _Q	b	R ² logC-logQ
$\text{NO}_3\text{-N}$	759	4.06 \pm 2.69 (3.71 \pm 3.14)	3.86 \pm 2.74 (3.4 \pm 3.2)	0.38 \pm 0.27 (0.29 \pm 0.27)	275 (274)	0.47 \pm 0.43 (0.33 \pm 0.34)	0.26 \pm 0.35 (0.16 \pm 0.36)	0.27 \pm 0.24 (0.22 \pm 0.41)
$\text{PO}_4\text{-P}$	695	0.12 \pm 0.12 (0.08 \pm 0.11)	0.10 \pm 0.10 (0.07 \pm 0.09)	0.68 \pm 0.33 (0.60 \pm 0.28)	261 (236)	0.70 \pm 0.42 (0.58 \pm 0.31)	-0.22 \pm 0.27 (-0.25 \pm 0.35)	0.21 \pm 0.19 (0.15 \pm 0.30)
TOC	722	5.88 \pm 2.96 (4.96 \pm 3.35)	5.33 \pm 2.81 (4.45 \pm 3.19)	0.41 \pm 0.16 (0.38 \pm 0.17)	256 (255)	0.49 \pm 0.33 (0.40 \pm 0.23)	0.18 \pm 0.22 (0.14 \pm 0.23)	0.19 \pm 0.20 (0.13 \pm 0.26)

Note: Given are the sample sizes n and the mean \pm standard deviation of the mean and median concentrations, the coefficients of variation of concentration CV_C and the metrics of C-Q relationships (i.e. CV_C/CV_Q, slope b with corresponding R^2). Values in brackets refer to median \pm interquartile range.

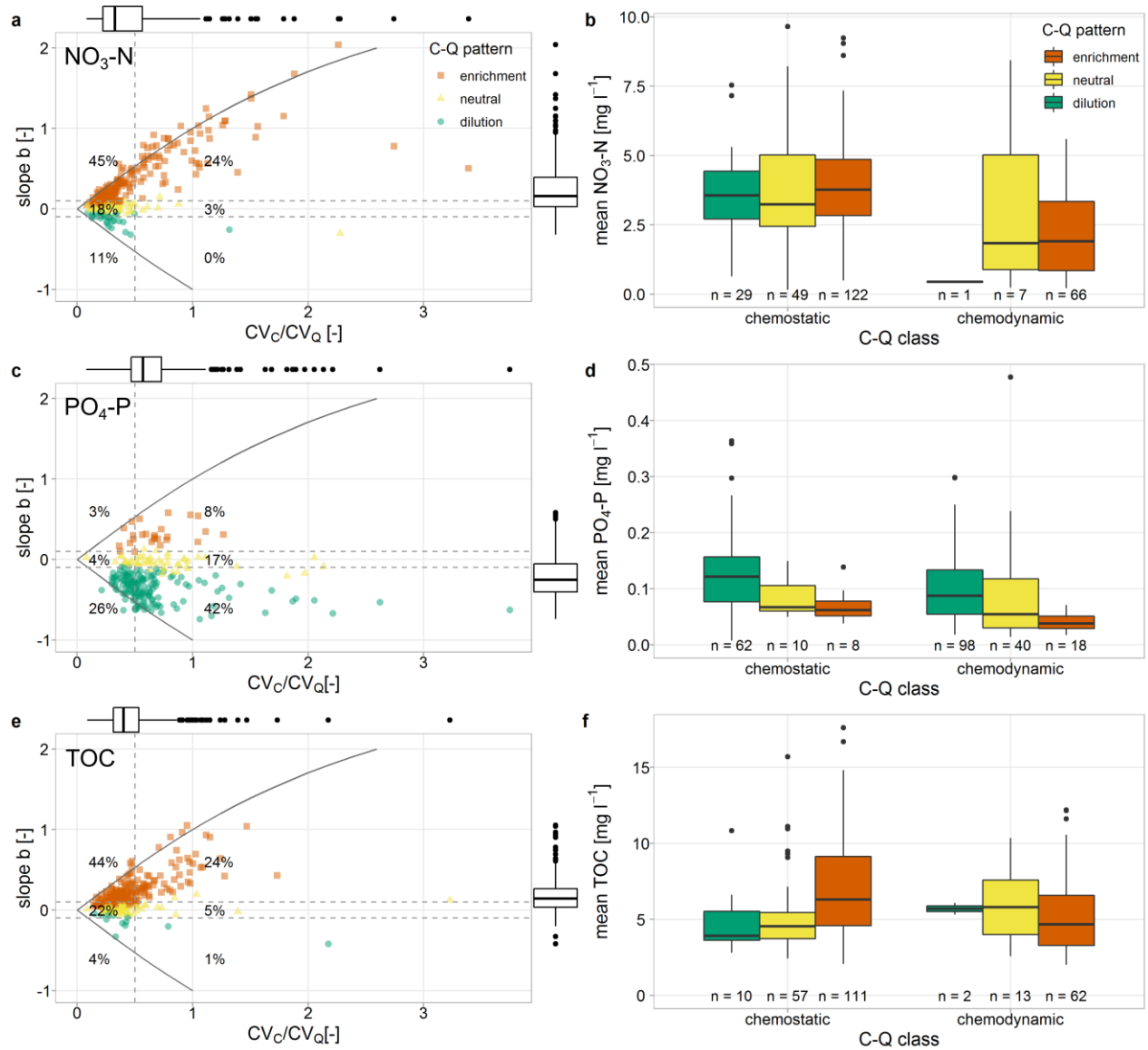


Figure 3. C-Q classification schemes composed of CV_c/CV_Q for export regimes and slope b for export patterns for NO_3-N (a), PO_4-P (c) and TOC (e) adapted from Musolff et al. (2015). Colors and shape indicate the class of C-Q patterns, horizontal dashed lines approximate these class divisions, while the vertical dashed line divides the two classes of C-Q regimes with $CV_c/CV_Q < 0.5$ for chemostatic and $CV_c/CV_Q > 0.5$ for chemodynamic regimes. The solid lines indicate the theoretical boundaries between slope b and CV_c/CV_Q for $CV_Q=0.6$ (after Musolff et al., 2015). Shown percentages indicate the portion of catchments assigned to the corresponding C-Q class. For each class mean concentrations of NO_3-N (b), PO_4-P (d) and TOC (f) are shown as boxplots. n - number of observations in this class.

The classification of nutrient export dynamics together with mean concentrations are shown in Figure 3.

For NO_3-N export, the majority of catchments showed a chemostatic regime (74 %, $n = 200$) and an enrichment pattern (69 %, $n = 188$), while 45 % combined both (see Figure 3a, b). Highest mean concentrations were observed for chemostatic regimes, while mean

concentrations of the group with chemodynamic regimes were significantly lower (Kruskal-Wallis, $p < 0.001$). The mean concentrations between the different C-Q patterns did not differ significantly.

For $\text{PO}_4\text{-P}$ export, the majority of catchments exhibited a chemodynamic regime (67%, $n=156$) and a dilution pattern (68%, $n=160$), while the combination of both can be found for 42% of all catchments (see Figure 3c, d). Independent of the C-Q pattern, mean concentrations were significantly lower in the chemodynamic compared to chemostatic regime (Kruskal-Wallis, $p < 0.001$). Among the C-Q patterns, mean concentrations were significantly higher for dilution patterns compared to neutral (Wilcoxon, $p = 0.002$) and to enrichment (Wilcoxon, $p < 0.001$) patterns. Catchments with enrichment patterns showed the lowest mean concentrations though they were not significantly different from catchments with neutral C-Q patterns (Wilcoxon, $p = 0.057$).

For TOC, chemostatic export (70 %, $n= 178$) and enrichment patterns (68 %, $n = 173$) prevailed with 44% of the catchments combining both (see Figure 3e, f). Overall, the chemostatic regime showed significantly higher mean TOC concentrations than the chemodynamic regimes (Kruskal-Wallis, $p = 0.014$). The mean concentrations between the C-Q patterns also differed significantly (Kruskal-Wallis, $p = 0.007$). The catchments with enrichment patterns had significantly higher mean concentrations than those exhibiting neutral C-Q patterns (Wilcoxon, $p = 0.011$), which was mainly apparent within the chemostatic regime (see Figure 3f).

3.2. Spatial Patterns of Concentrations and Export Dynamics

The spatial organisation of mean concentrations and export patterns of each nutrient are shown in Figure 4. For all nutrients, regional clusters of the export patterns can be observed. $\text{NO}_3\text{-N}$ showed the strongest enrichment patterns in Northern Germany and some dilution patterns in South-West Germany. The highest mean $\text{NO}_3\text{-N}$ concentrations were found in the Eastern part of Germany. TOC also showed strong enrichment patterns in Northern Germany, esp. in the North-West, but also in the South of Germany, while the small amount of dilution patterns seemed to cluster more in the Central-West. The highest mean TOC concentrations were found in the lowlands in Northern, esp. North-Western Germany coinciding with the enrichment patterns. For $\text{PO}_4\text{-P}$, the few enrichment patterns clustered in the North-West and South-East of Germany. Highest mean $\text{PO}_4\text{-P}$ concentrations were found in Central-Germany, though a general spatial organisation was not obvious for this metric.

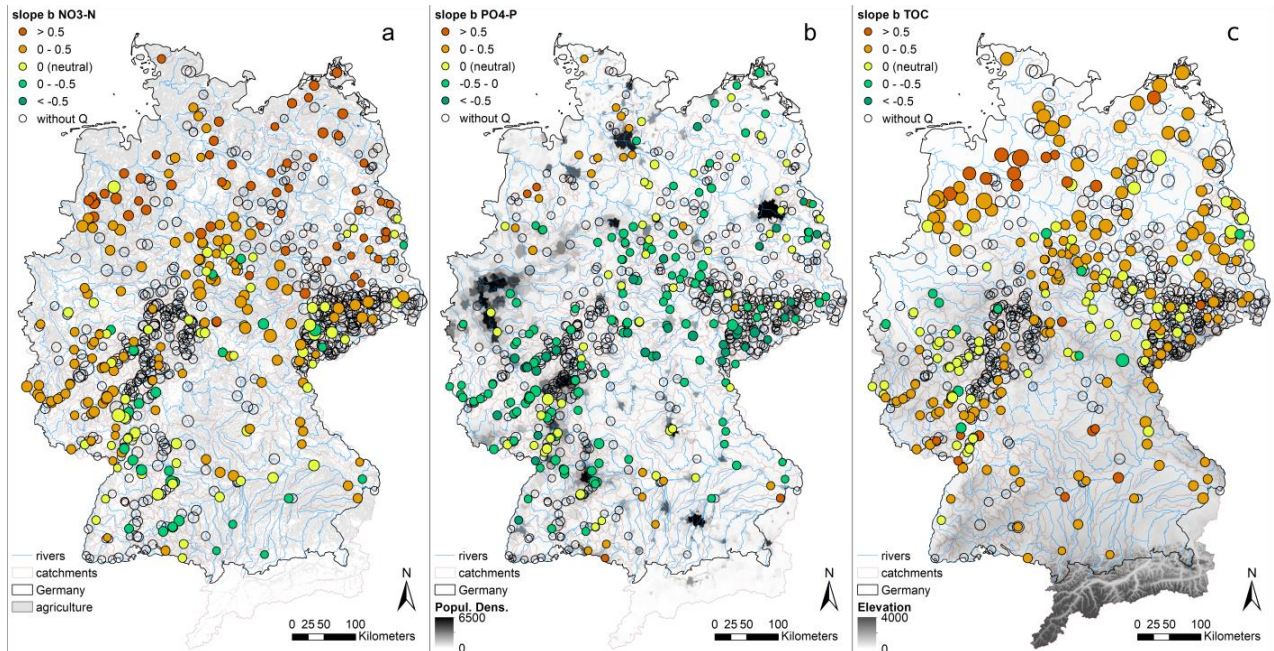


Figure 4. Spatial patterns of C-Q slope b across Germany with point size relative to mean concentrations (scaled to the respective range) for $\text{NO}_3\text{-N}$ (a), $\text{PO}_4\text{-P}$ (b), and TOC (c).

3.3. Relationships Among the Nutrient Export Metrics

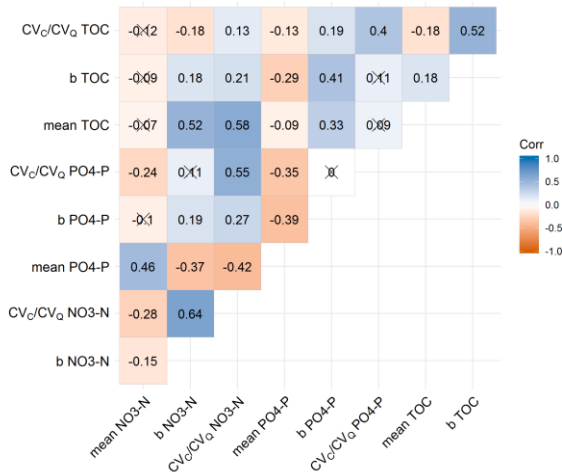


Figure 5. Spearman rank correlation matrix between metrics of the export regimes. Crosses mark non-significant correlations (significance level of 0.05)

To describe interactions between the three major nutrients, we quantified the interdependencies between the water quality metrics using spearman rank correlations (Figure 5). For $\text{NO}_3\text{-N}$ and $\text{PO}_4\text{-P}$, all metrics correlated positively, which was strongest for CV_c/CV_Q ($r=0.55$) and lowest for slope b ($r=0.19$). For $\text{NO}_3\text{-N}$ and TOC, mean TOC correlated positively with the $\text{NO}_3\text{-N}$ export metrics (CV_c/CV_Q $r=0.58$ and slope b $r=0.52$), which was also apparent for the respective TOC export metrics but less pronounced. For $\text{PO}_4\text{-P}$ and TOC, slope b of $\text{PO}_4\text{-P}$ correlated positively and mean $\text{PO}_4\text{-P}$ concentration negatively with all TOC metrics, with the

correlation coefficient between the slopes b being the highest ($r=0.41$). This was similar to the correlation coefficient between the CV_C/CV_Q of $PO_4\text{-P}$ and TOC ($r=0.4$).

3.4. Linking Export Metrics to Catchment Characteristics

Several co-linearities exist among the catchment characteristics quantified for all variables by Spearman rank correlations (for correlation matrix see Figure S3). The land cover classes fraction of agriculture and forest were strongly negatively correlated as opposing land use classes. Agricultural land fraction also correlated negatively with the topographic slope, water available in the root zone, the C/N ratio and N content in the topsoil and positively with N surplus and soil P content. The topographic variables were strongly correlated among themselves such that higher slopes prevailed in higher elevations and linked to lower TWI. Topography variables also correlated with descriptors of climate and hydrology (e.g., higher topographic slopes related to higher precipitation amount and frequency, specific discharge, runoff coefficient and discharge variability but lower aridity index), lithology (e.g., higher slopes related to lower fractions of sedimentary aquifers and lower depth to bedrock), soil chemistry (e.g., higher slopes related to higher N in the topsoil but less P) and source heterogeneity (e.g., higher slopes related to lower mean source distances to stream and lower vertical concentration contrasts). This means that flat lowland catchments tend to have more agriculture and diffuse sources, more sedimentary aquifers with deeper bedrock, more riparian wetlands and more vertical concentration contrasts but lesser precipitation and lesser discharge.

Correlations between the response metrics and individual catchment characteristics are given in the Figure S4. They provide a first indication of existing links between the characteristics and the responses, e.g. between the topography and the mean TOC concentration and the C-Q relation metrics of $NO_3\text{-N}$. Yet, due to correlations among several descriptors suitable multivariable statistical approaches were required for interpretation of linkages and hierarchies (see Section 2.4) of which the results are presented in the following section.

3.4.1. Predictive Power of Descriptors for Response Variables

The descriptor variables for horizontal source heterogeneity ($sdist_mean$, het_h) did neither prove to be among the significant predictors nor improve the model performances of the PLSR and RF models (PLSR and RF results presented in Table S3-S4) nor correlate strongly with the export metrics (Figure S4). As missing values for these variables, described earlier in Section 2.3, reduced the overall number of catchments usable for PLSR and RF, we decided to redo the analysis with the bigger sample size excluding these variables. The set of catchments presented in Section 2.3 and results consistently refer to this larger selection.

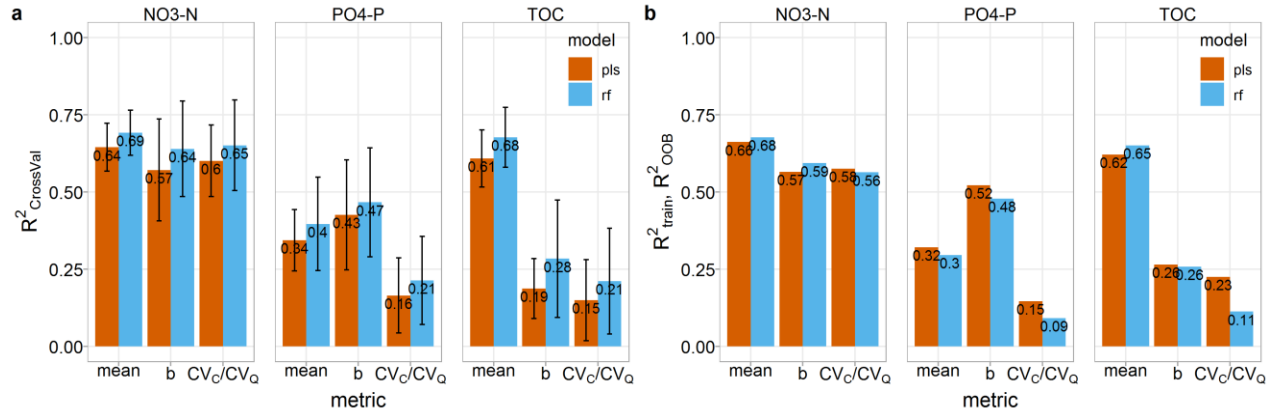


Figure 6. PLSR and RF model performances as mean R^2 of the cross-validation with error bars indicating the standard deviations among the 30 cross-validation folds (a) and of the trained models calculated from out-of-bag samples for RF (b).

The variability in the C-Q metrics could be explained by the catchment characteristics, however, to different degrees depending on the nutrient types and their descriptive metrics (Figure 6). The mean R^2 in cross-validation were consistently higher for the RF models, but not substantially, considering the apparent variability between the different folds. The model performances of the trained models, R^2_{train} for PLSR and R^2_{OOB} for RF models, generally reached similar levels compared to the cross-validation. Note that the R^2_{OOB} is calculated based on out-of-the-bag samples in the RF models and thus not directly comparable to R^2_{train} of the PLSR models.

All three NO_3 -N metrics could be predicted with a reasonably good cross-validated performance, $R^2_{CrossVal} > 0.5$ with the highest value being $R^2_{CrossVal} = 0.69$ for mean NO_3 -N concentrations with RF. For PO_4 -P, performance is substantially lower. Models for mean concentrations reached $R^2_{CrossVal} > 0.3$ and slope b $R^2_{CrossVal} > 0.4$, while the models CV_c/CV_q of PO_4 -P only reached $R^2_{CrossVal} < 0.3$. For TOC, mean concentrations were well explained with $R^2_{CrossVal} > 0.5$, while the C-Q metrics CV_c/CV_q and slope b in contrast only reached $R^2_{CrossVal} < 0.3$. The model results provide variable importance measures that allow ranking the descriptive power of the catchment characteristics within the explained variability of the response (Table 3 presents variables with highest ranks, Table S5-S7 the complete results). For models with low overall explained variability the interpretation of variable importance is very limited though.

For mean NO_3 -N concentrations, both PLSR and RF models rank the fractions of forest highest relating to low diffuse inputs, followed by agricultural land cover and top soil C/N ratio in PLSR and mean annual precipitation and its seasonality in RF. In the PLSR model, there is a prominent difference in variable importance to the next descriptors vertical source heterogeneity, fraction of sand and clay (all three with a positive direction of influence) and the fraction of sedimentary aquifer. The RF model marks a step in variable importance after the first ranked fraction of forest, which is followed by mean annual precipitation and its seasonality, fraction of sedimentary aquifer, mean vertical heterogeneity and the fraction of agriculture on rank 6. For explaining the NO_3 -N dynamics (b and CV_c/CV_q) the descriptor vertical heterogeneity has the highest importance (ranks highest in three of the four models). The PLSR model coefficients indicate a positive link meaning that the slope b tends to be higher in areas with high vertical

contrast between potential seepage and groundwater NO₃-N concentrations. Only the RF model ranks the topographic descriptors (slope_mean, twi_mean, dem_mean) highest for the slope b of NO₃-N, which also appear relatively high ranked in the other three models for NO₃-N export dynamics following het_v. The variables depth to bedrock (dtb) and fraction of sedimentary aquifer (f_sedim) also obtain high importance values.

For mean PO₄-P concentrations, the P load from point sources stands out with the highest variable importance in both models and a large step to the second ranked variables. Slope b of the C-Q relationship is explained the most by mean N surplus (N_surp_00 and N_surp_80) and the fraction of sedimentary aquifers, all with a positive relation to b. After a step in variable importance, these three variables are followed by the 90th percentile of the TWI, the P content in the topsoil and the precipitation frequency, amount and seasonality.

Mean TOC concentrations are explained the most by the TWI (90 percentile and mean) based on PLSR and by mean elevation and topographic slope based on RF. The other respective topographic variables as well turn out highly ranked in the other model together with the fraction of sedimentary aquifers, potential evapotranspiration and depth to bedrock.

Table 3. Ranked Drivers and Model Performances of PLSR with VIP and RF for the Three Nutrients and Metrics.

Res- ponse	Mean concentration				b				CV _C /CV _Q			
NO ₃ -N	n=759				n=274				n=275			
	PLSR R ² _{CrossVal} =0.64 R ² _{train} =0.66			RF R ² _{CrossVal} =0.69 R ² _{OOB} =0.68	PLSR R ² _{CrossVal} =0.57 R ² _{train} =0.57			RF R ² _{CrossVal} =0.64 R ² _{OOB} =0.59	PLSR R ² _{CrossVal} =0.60 R ² _{train} =0.58			RF R ² _{CrossVal} =0.65 R ² _{OOB} =0.56
	Variable	VIP	Sig n	Variable Imp	Variable	VIP	Sig n	Variable Imp	Variable	VIP	Sig n	Variable Imp
	f_forest	1.93	-	f_forest 20.3	het_v	1.66	+	slope_mean 11.5	het_v	1.70	+	het_v 10.2
	f_agric	1.88	+	P_mm 17.4	twi_mean	1.55	+	twi_mean 11.2	f_sedim	1.58	+	twi_mean 9.3
	soil_CN	1.82	-	P_Slsw 16.2	dtb	1.48	+	dem_mean 9.0	dtb	1.42	+	slope_mean 9.3
	het_v	1.40	-	f_sedim 15.8	f_sedim	1.48	+	soil_N 8.1	f_silt	1.40	-	dem_mean 7.4
	f_sand	1.38	+	het_v 14.4	twi_90p	1.47	+	PET_mm 7.7	twi_mean	1.37	+	f_sedim 6.9
	f_clay	1.32	+	f_agric 13.9	dem_mean	1.46	-	P_mm 7.3	f_sand	1.36	+	soil_N 6.6
PO ₄ -P	n=695				n=236				n=261			
	PLSR R ² _{CrossVal} =0.34 R ² _{train} =0.32			RF R ² _{CrossVal} =0.40 R ² _{OOB} =0.30	PLSR R ² _{CrossVal} =0.43 R ² _{train} =0.52			RF R ² _{CrossVal} =0.47 R ² _{OOB} =0.48	PLSR R ² _{CrossVal} =0.16 R ² _{train} =0.15			RF R ² _{CrossVal} =0.21 R ² _{OOB} =0.09
	Variable	VIP	Sig n	Variable Imp	Variable	VIP	Sig n	Variable Imp	Variable	VIP	Sig n	Variable Imp
	P_WW	2.04	+	P_WW 23.1	N_surp_00	1.82	+	f_sedim 15.0	f_sedim	1.79	+	T_mean 6.8
	f_artif	1.71	+	dem_mean 9.2	N_surp_80	1.73	+	N_surp_00 13.1	f_sand	1.58	+	thetaS 5.8
	soil_CN	1.67	-	f_silt 8.9	f_sedim	1.61	+	N_surp_80 12.7	het_v	1.55	+	twi_mean 5.6
	pdens	1.60	+	PET_mm 8.2	twi_90p	1.36	+	P_lambda 9.3	dtb	1.54	+	WaterRoots 5.5
	PET_mm	1.53	+	f_silic 7.4	soil_P	1.35	+	twi_90p 9.2	f_silt	1.51	-	dem_mean 5.2
	f_sand	1.53	-	dtb 7.3	P_mm	1.35	+	P_Slsw 8.6	f_water	1.44	+	slope_mean 4.7
TOC	n=722				n=255				n=256			
	PLSR R ² _{CrossVal} =0.61 R ² _{train} =0.62			RF R ² _{CrossVal} =0.68 R ² _{OOB} =0.65	PLSR R ² _{CrossVal} =0.19 R ² _{train} =0.26			RF R ² _{CrossVal} =0.28 R ² _{OOB} =0.26	PLSR R ² _{CrossVal} =0.15 R ² _{train} =0.23			RF R ² _{CrossVal} =0.21 R ² _{OOB} =0.11
	Variable	VIP	Sig n	Variable Imp	Variable	VIP	Sig n	Variable Imp	Variable	VIP	Sig n	Variable Imp
	twi_90p	1.71	+	dem_mean 14.2	N_surp_00	1.55	+	f_sedim 11.8	f_sedim	1.43	+	drain_dens 8.9
	twi_mean	1.71	+	slope_mean 13.1	N_surp_80	1.46	+	N_surp_00 10.9	f_silic	1.36	-	f_calc 8.5
	f_sedim	1.57	+	twi_mean 13.1	f_sedim	1.43	+	N_surp_80 8.6	soil_N	1.34	-	f_silt 7.7
	slope_mean	1.46	-	twi_90p 12.0	f_silic	1.37	-	dem_mean 8.3	f_calc	1.33	+	P_Slsw 7.1
	dem_mean	1.37	-	PET_mm 11.0	het_v	1.27	-	f_silt 8.0	T_mean	1.33	+	soil_P 5.8
	dtb	1.36	+	f_sedim 9.9	AI	1.18	-	P_mm 7.8	f_gwsoils	1.31	-	P_mm 5.6

Note: Only the six highest ranked variables are shown, the complete results are given in Table S6-8 in the supporting information. CrossVal - cross-validation; OOB – out-of-bag samples; VIP - variable influence on projection of PLSR; Imp – variable importance in RF models.

4 Discussion

4.1. Nutrient-Specific Export and Controls

4.1.1. NO₃-N: Natural Attenuation Buffers Input and Controls Export Regimes

For NO₃-N export in the study catchments, we found a dominance of enrichment patterns and chemostatic regimes and significantly higher mean concentrations for chemostatic compared to chemodynamic regimes.

The variability in mean NO₃-N concentrations among the studied catchments was linked to the land use as the fractions of forest and of agriculture both ranked high in the PLSR and RF models and relate to low and high diffuse N sources, respectively. The fraction of either forest or agriculture alone could explain 32% or 29% of this variability in a simple linear regression respectively, while in the PLSR and RF the total variability explained by all descriptors was 64 to 70%. Interestingly, the N surplus could only explain 3.5% for N_surp_00 and 6.4% for N_surp_80 in a simple linear model even though it is strongly related to agricultural land (f_agric and N_surp_00 $r=0.58$, and N_surp_80 $r=0.71$, spearman rank, Figure S3). Probably, this is related to a few catchments with exceptionally high N surplus but moderate mean NO₃-N concentrations.

However, the relationship between the fraction of agriculture and the mean NO₃-N concentration is highly heteroscedastic as shown in **Figure 7**. We found that deviations from a positive linear relationship between N input and N output are related to soil and aquifer properties as e.g. f_sedim ranked high in the PLSR and RF (Table 3 and S5), which could indicate buffering of inputs by natural attenuation (removal by denitrification). Adding the fraction of sedimentary aquifer as a secondary factor to the linear model with forest (or agriculture) fractions increased the explained variability to 52% (or 49%) respectively. Previous studies have shown that sedimentary aquifers often exhibit high denitrification potential (Hannappel et al., 2018; Knoll et al., 2020; Kunkel et al., 2004). Unconsolidated aquifers are usually deep low-land aquifers linked to long travel times (Merz et al., 2009; Wendland et al., 2008) with anaerobic conditions, organic carbon or pyrite deposits providing electron donors for denitrification, especially in the lowlands of Northern Germany (Kunkel et al., 2004; Wendland et al., 2008). Both long residence times and favourable conditions for denitrification increase the potential for NO₃ removal along the flow path (Rivett et al., 2008). This link is supported by het_v, ranked 4th and 5th, which represents the vertical concentration contrast, likely resulting from denitrification under anaerobic subsurface conditions (Knoll et al., 2020) and correlating positively with f_sedim ($r=0.68$). Denitrification in riparian wetlands, more abundant in lowlands, could additionally buffer NO₃-N inputs and create a link to the carbon cycle (see also Section 4.2) (Lutz et al., 2020; Pinay et al., 2015; Sabater et al., 2003). Instead of effective N removal by denitrification, the decrease in concentration could also be linked to the large groundwater storages of deep sedimentary aquifers causing high dilution by old (pre-industrial) water fractions low in NO₃-N concentrations and resultant vertical concentration contrasts. In this case, the system would not be equilibrated in terms of its N balance within the investigated time frame (Ehrhardt et al., 2019). Additionally, instream retention could also be higher in areas with low slopes due to longer residence times in the river network.

As a third component and climatic driver, the seasonality of precipitation could slightly increase the variability of mean NO₃-N explained to $R^2 = 55\%$ in combination with f_forest (53% with f_agric) in a linear regression though the high ranking in RF but not in PLSR suggests rather a non-linear relation. Higher precipitation seasonality P_SIs_w, i.e. higher summer to winter precipitation, was linked to higher mean NO₃-N. Possibly, areas with higher P_SIs_w have a lower dilution potential of NO₃-N loads especially during winter, typically the season of high riverine NO₃-N concentration. Moreover, high P_SIs_w prevail in areas of lower mean precipitation P_mm ($r=-0.51$, spearman rank) and higher aridity index (AI; $r=0.49$) decreasing the overall hydro-climate related dilution potential.

Altogether, this clearly indicates that the anthropogenic N-input from diffuse sources is a first order control for mean $\text{NO}_3\text{-N}$ concentrations observed in the surface water, while natural attenuation is able to buffer the high inputs especially in lowlands with deep aquifers, whereas hydroclimatic conditions seem to play a subordinate role.

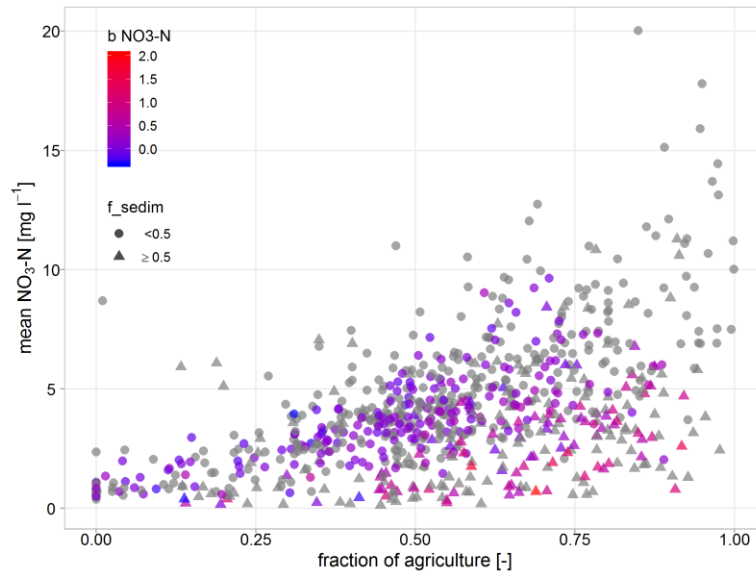


Figure 7. Relation between the fraction of agriculture as diffuse source of N, mean $\text{NO}_3\text{-N}$ concentrations. Colors indicate the slope b of C-Q relationship and the shape indicates if sedimentary aquifer type dominates.

In this study, high mean $\text{NO}_3\text{-N}$ were often combined with low concentration variability (**Figure 3**), i.e. chemostatic regimes ($\text{CV}_C/\text{CV}_Q < 0.5$), and neutral C-Q patterns ($b \approx 0$). This finding agrees with Thompson et al. (2011) who found significantly lower CV_C/CV_Q for the group of catchments with higher $\text{NO}_3\text{-N}$ export and hypothesized that such behaviour was due to homogenization of sources. Minaudo et al. (2019), on the other hand, found that the background pollution level, an indicator for mean $\text{NO}_3\text{-N}$ concentrations, was positively correlated to the seasonal $\text{NO}_3\text{-N}$ dynamics (i.e. slope b). This study disagrees with the hypothesis that highly-managed, agricultural catchments are subject to homogenization of sources and thus to chemostatic export regimes (Basu et al., 2010) as high fractions of agriculture did not induce chemostasis and neutral C-Q patterns. Instead, many agriculture dominated catchments exhibited chemodynamic export with enrichment patterns and relatively low mean concentrations (**Figure 7**). These chemodynamic catchments widely coincided with catchments where sedimentary aquifers and strong vertical concentration heterogeneity prevailed.

The variability in the export dynamics, i.e. regimes and patterns, were mostly explained by and positively linked to the descriptor het_v representing the average vertical $\text{NO}_3\text{-N}$ heterogeneity from soils to groundwater within each catchment. In contrast, the variables of horizontal source heterogeneity het_h and sdist_mean did not show a dominant effect. This means the larger the downward concentration decrease is over depth, the more dynamic and enriching $\text{NO}_3\text{-N}$ is exported, and the smaller the gradient, the more chemostatic the export. Accordingly, our results from data-driven analysis over a wide range of catchments confirm findings from previous modeling studies: Zhi et al. (2019) found vertical concentration gradients resulting from source distributions and reactions in combination with end-member mixing and

Musolff, Fleckenstein, et al. (2017) found the concentration gradient over travel times as a more general, indirect measure of solute source heterogeneity to control C-Q patterns. The linkage between vertical concentration heterogeneity and export patterns seems plausible, as agricultural and atmospheric N input enter the subsurface from the top. A top-loaded profile in combination with the dominance of young water contribution to discharge from upper soil layers during high flows, and dominance of old water fractions at base flow conditions (exponential saturated hydraulic conductivity profile) causes a positive C-Q slope. This interpretation coincides with the concept of juxtaposition of discharge generation and concentration profiles by Seibert et al. (2009) and with the scenario of higher concentrations linking to shorter travel times in Musolff, Fleckenstein, et al. (2017). On a longer term, the concentration gradient will only be retained when subsurface attenuation occurs. Note that if discharge generating zones are stationary over time, chemostasis can also be generated from a heterogeneous profile.

We found that the interaction between diffuse input and reactivity, more specifically the combined effect of reaction rates and residence times along the flow paths resulting in $\text{NO}_3\text{-N}$ attenuation, might determine the strength of vertical concentration heterogeneity. Consequently, chemodynamic export with enrichment patterns could indicate natural attenuation and effective denitrification under high inputs. In consequence, chemostasis would be rather explained by missing reactivity of the catchment than by the existence of large legacy N pools in the catchments, as previously suggested (Basu et al., 2010), although both may co-exist. Chemodynamic export may also occur when vertical concentration contrasts emerge from the existence of $\text{NO}_3\text{-N}$ poor older water fractions in large and deep groundwater bodies. The consistent relationship between input, attenuation and export patterns (**Figure 7**) also suggests that catchments with relatively low mean $\text{NO}_3\text{-N}$ concentrations but high inputs and steep positive C-Q patterns might still be “hot spots” in terms of exported loads, eutrophication risk, and large N legacies. Here, the natural attenuation might effectively buffer inputs in terms of mean riverine and groundwater concentrations but not necessarily the exported loads during high-flows. The denitrification capacity could however decrease or exhaust over time when electron donors are consumed, which has been discussed, for example, by Wilde et al. (2017) and Hannappel et al. (2018). Additionally, tile drainages can enhance the effect of concentration heterogeneity by increasing the younger water during high-flows and avoiding potential retention zones (Musolff et al., 2015; Van der Velde et al., 2010; Van Meter & Basu, 2017). As geoinformation on drainages over this large scale is not available we cannot prove the role of this additional flow path in this study. Still, drainage systems are the main delivery pathway of N into surface waters in Mecklenburg-Vorpommern contributing 70% of the total N input (Kunkel et al., 2017) and widely spread in Germany (Behrendt, 1999) (see also Section 4.1.2).

4.1.2. $\text{PO}_4\text{-P}$: Unexpected Dominant Control of Diffuse Sources on Export Patterns

For $\text{PO}_4\text{-P}$ export, dilution patterns with chemodynamic regimes prevailed (42% of the study catchments), while the dilution group had the highest mean concentrations. Mean $\text{PO}_4\text{-P}$ concentrations were positively linked to direct anthropogenic input from point sources to the streams although, surprisingly, overall explained variance in the PLSR and RF models was low ($R^2_{\text{CrossVal}} = 0.34$ and 0.40). A linear regression of mean $\text{PO}_4\text{-P}$ and P_WW confirmed that its descriptive power was weak ($R^2 = 11\%$). In combination with a second variable, selected based on rankings in PLSR and RF models, the linear models with the topsoil C/N ratio explained 20% (soil_CN) and with a climatic descriptor explained 19% (AI), 18% (T_mean) and 17% (PET_mm). Previous studies also state the dominant role of point sources for average riverine

total P concentrations (Minaudo et al., 2019; Westphal et al., 2019; Withers & Jarvie, 2008), with contributions remaining high even after significant reductions of inputs from point sources (Behrendt, 1999; Westphal et al., 2019).

In general, $\text{PO}_4\text{-P}$ is subject to P cycling caused by highly dynamic, small-scale biotic and abiotic processes, including retention and remobilization processes in the stream (Withers & Jarvie, 2008). By this, P cycling potentially reshapes direct inputs and delivery from land-stream transfer at catchment scale. This could explain that mean $\text{PO}_4\text{-P}$ concentrations are linked to the inputs but hardly predictable by average catchment characteristics because factors affecting instream nutrient retention, transformation and remobilization are not adequately represented (Withers & Jarvie, 2008; Withers et al., 2012). These factors include physico-chemical and biological controls such as redox conditions, mineral precipitation and dissolution, water temperatures, river bed morphology and biological uptake and mineralisation, which may vary strongly in space and time (Withers & Jarvie, 2008). Other reasons could be uncertainties related to (1) the point source data disregarding potential intra- and interannual variability, or (2) the sampling frequency of C potentially missing moments of peak concentrations and leading to underestimation of mean $\text{PO}_4\text{-P}$, as noted by e.g. Hunsaker and Johnson (2017).

For $\text{PO}_4\text{-P}$ export dynamics, dilution patterns prevailed in two thirds of the catchments which agrees with previous studies and has usually been associated with point-source dilution (Dupas, Gascuel-Oudoux, et al., 2015; Moatar et al., 2017; Musolff et al., 2015) or biogeochemical processes releasing $\text{PO}_4\text{-P}$ during summer low-flows and thus mimicking point sources (Dupas et al., 2018). Enrichment patterns of $\text{PO}_4\text{-P}$, which have been found in just 11% of the catchments, have also been observed in other cases, e.g. during storm events in agricultural settings by Rose et al. (2018) and Bieroza and Heathwaite (2015), who explain this by dominance and mobilization of diffuse sources. Similar behaviour was noticed in forested catchments by Hunsaker and Johnson (2017), who explain the $\text{PO}_4\text{-P}$ enrichment by mobilization from a nutrient-rich O-horizon under high-flows linking soil to water chemistry.

Interestingly, even with prevailing dilution patterns, not the amount of point source derived P in the catchment, but instead the N surplus and fraction of sedimentary aquifers turned out to be the most dominant predictive variables and were positively linked to slope b. Both variables together explain 42% of the variability in slope b of $\text{PO}_4\text{-Q}$ relationships in a linear model, and individually 27% and 26% respectively. This constitutes a large part of the explained variability of all descriptors (R^2_{CrossVal} spans 0.43-0.47). This high relatively predictive power of N surplus is explained by the catchments with very high N surplus exhibiting positive C-Q relationships.

Especially in North-West and South-East Germany, catchments with high N surplus tended to show enrichment patterns for $\text{PO}_4\text{-P}$ (Figure 4), i.e. higher $\text{PO}_4\text{-P}$ concentrations with higher discharge. High P applications, especially from manure, and low P use efficiencies have led to widespread P accumulation on agricultural soils increasing the risk of P losses (Schoumans et al., 2015). Sharpley et al. (2013) explain that P legacies can cause saturation of soil sorption capacities resulting in P mobilization in contrast to the usual predominance of the solid phase and sorption. In field experiments, Hahn et al. (2012) observed that manure applications and soil P status additively increased diffuse P losses. As areas with prevailing enrichment patterns coincide with regions of intense manure applications from livestock farms (Häußermann et al., 2019) and high degrees of P saturation (Fischer et al., 2017), they are probably the reason for the enhanced $\text{PO}_4\text{-P}$ land-to-stream transfer. This is supported by the PLSR model in which topsoil P

content (soil_P) links positively to slope b and ranks order 5. Fischer et al. (2017) found widespread (>76%) high risks of dissolved P loss from German agricultural soils, so that this process of diffuse P mobilization is likely to occur in more than 11% of the catchments but might be less dominant in catchments where dilution prevails.

Tile drainages and preferential flow paths can enhance P transfer to streams because P from upper soil layers can bypass the potential sinks in the soil matrix and P accumulation can additionally be enhanced along those flow paths (Sharpley et al., 2013). Tile drainage can increase exported P (Rozemeijer et al., 2010) and cause positive $\text{PO}_4\text{-Q}$ relationships (Gentry et al., 2007). This means that tile drainages have the potential to translate existing spatial source heterogeneity between top and deeper soil and aquifer layers into stream water quality dynamics by avoiding reactive zones and that this mechanism could be activated before widespread soil P saturation. Artificial drainages are likely to be present in those parts of Germany to facilitate agricultural production on flat areas and relatively wet soils, which might partly be related to the high ranks of f_{sedim} and $\text{twi}_{90\text{p}}$ with positive coefficients in the PLSR. For Germany, the fraction of artificially drained areas of agricultural land has been estimated to 12.4% (Behrendt, 1999), while the fractions can be higher in single catchments, especially in the north western Germany with e.g. 41% in the Weser catchment (Tetzlaff et al., 2009), but also in eastern Germany e.g. 21.7% in the Mulde catchment (Behrendt, 1999).

Assuming that N surplus and top soil P represent diffuse anthropogenic P inputs, our PLSR and RF results suggest that P mobilization is facilitated by diffuse P inputs, high degrees of P saturation and potentially preferential flowpaths, including artificial drainage systems, and is likely to cause the observed enrichment patterns and be a dominant process in agricultural landscapes. P saturation in the topsoil can be considered as source heterogeneity with a top-loaded profile.

Climatic controls were also identified and ranked relatively high in both PLSR and RF models, e.g. mean annual precipitation showed a positive impact on slope b (Figure 8, Table 3). The PLSR and RF models including hydrological descriptors indicate that a higher seasonal Q ratio ($\text{seasRQ} \approx 1$, i.e. higher summer compared to winter Q and more equilibrated Q seasonality) relates to a higher slope b and takes over the rank of P in these models (Table S7). This suggests that the impact of higher P is related to a higher dilution potential especially during the summer low-flow period. A higher summer discharge causes lower concentrations during low-flow period and thus less $\text{PO}_4\text{-P}$ dilution export patterns. In general, high precipitation amounts could also favour reducing conditions for $\text{PO}_4\text{-P}$ mobilization or a higher potential of land-stream transfer of diffuse P sources especially during high-flows. Though the latter is not apparent in the data as extreme seasonality with relatively high winter Q ($\text{seasRQ} \ll 1$) should then enhance enrichment patterns, but higher seasRQ and P consistently link to higher slope b values. The climatic dilution component creates additional variability between sources and exported concentrations.

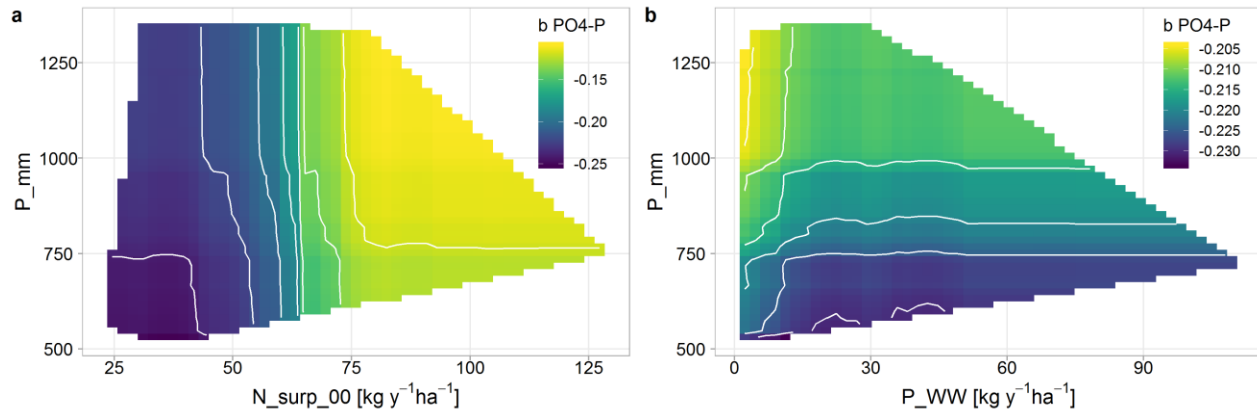


Figure 8. Partial dependence plots for RF model for slope b of $\text{PO}_4\text{-P}$ showing the interaction between a) N surplus ($N_{\text{surp_00}}$) and b) P loads from point sources (P_{WW}) with mean annual precipitation (P_{mm}). Colors indicate the range of predicted b values with mean values for the other descriptors. White areas are outside the covered parameter space (without extrapolation).

Figure 8 confirms that the impact of N surplus on slope b exceeds the impact of point sources and climatic drivers (as indicated by the steeper color gradient and value range in panel a). The impact of point sources is slightly visible for low loads suggesting slight threshold behaviour (Figure 8b): if there is any point source in the catchment, slope b tends to be smaller, i.e. more dilution patterns, while the magnitude of the source seems to be less important and the effect relatively weak.

All in all, the fact that slope b correlates negatively with mean $\text{PO}_4\text{-P}$ concentrations ($r=-0.39$, spearman rank, see Figure 5) and with point sources ($r=-0.2$, spearman rank, Figure S4) while point sources partly explain mean concentrations, suggests that point sources still influence $\text{PO}_4\text{-P}$ export dynamics even though their link is not strong. This fits to the hypothesis that P cycling significantly reshapes P responses by decoupling $\text{PO}_4\text{-P}$ concentrations from Q while keeping the $\text{PO}_4\text{-P}$ variability high, leading to the poor explanatory power of point sources and other averaged catchment characteristics used in this study. Moreover, point source inputs could be decoupled stronger than diffuse inputs because P cycling is likely more pronounced and variable during summer. This could be the reason why point sources have an influence on export patterns and dilution patterns prevail even though diffuse sources explain the overall variability of slope b better because the highest N surplus values relate to observed enrichment patterns.

4.1.3. TOC: Flat Topography Strengthens Sources and Hydrology-Driven Export

Topography related characteristics appeared to dominantly control mean TOC, as the TWI and the topographic slope turned out to be the dominant descriptors in PLSR and RF models with similar variable importance. The 90 percentile and the mean of TWI were good predictors, each alone explaining 52% of the variability in a linear model, while the mean elevation and slope ranked highest in the RF model, they explain less variability in a linear model (33 and 38% respectively). This topography control agrees with previous results by Zarnetske et al. (2018) who found the topographic slope and the share of wetlands followed by mean annual precipitation to best predict DOC concentrations levels in the contiguous US. Recently, Musolff et al. (2018) also found the 90 percentile of the TWI as a good predictor for median DOC concentrations in small mountainous, mainly forested German catchments. The 90

percentile of the TWI can also be interpreted as proxy for the extent of riparian wetlands (Musolff et al., 2018), source areas of organic matter and thus TOC. Higher twi_90p link to higher but also more variable mean TOC concentrations, resembling a heteroscedastic relationship (**Figure 9a**), similar to results by (Musolff et al., 2018) and over a wider range of topographic settings as presented in Musolff et al. (2015).

For TOC export, most catchments classified as enrichment patterns and chemostatic regimes. The dominance observed across Germany agrees with previous studies on the dominance of enrichment patterns and transport-limited export for DOC and TOC (Moatar et al., 2017; Musolff et al., 2018; Musolff et al., 2015; Zarnetske et al., 2018). Zarnetske et al. (2018) found wetland cover to control this patterns, while Musolff et al. (2018) found high twi_90p, soluble reactive phosphorus, pH and AI to relate to high C variability (as interquartile C range). The observed variability in the export metrics as noticed over the large set of study catchments could not be explained satisfactorily ($R^2_{\text{CrossVal}} \leq 0.28$) by the used characteristics, which include the fraction of wetland, the twi_90p and climatic characteristics. In Moatar et al. (2017), DOC-Q slopes correlated with various hydrological variables and, in Musolff et al. (2015), the variability in TOC dynamics were explained well by the BFI (+), artificial drainages (-) and topographic slope (+). In agreement, including the hydrological parameters as descriptors (Table S11) substantially increased the variance explained by the PLSR and RF models for the smaller number of study catchments with continuous daily Q time series between 11 and 37 % (with $R^2_{\text{CrossVal}} = 0.44$ for slope b in RF and $R^2_{\text{CrossVal}} = 0.58$ for CV_C/CV_Q in PLSR). Especially the flashiness index, seasonal ratio of discharge and BFI ranked high with a positive direction of influence suggesting that catchments with more equilibrated discharge patterns, i.e. less flashy, similar summer and winter discharge (seasRQ close to 1) and higher base flow, tend to mobilize TOC more dynamically with discharge but also show a higher variability in the export patterns (**Figure 9b, c**). Our analysis revealed hydrologic variables to be the dominant predictors controlling TOC dynamics across the study catchments

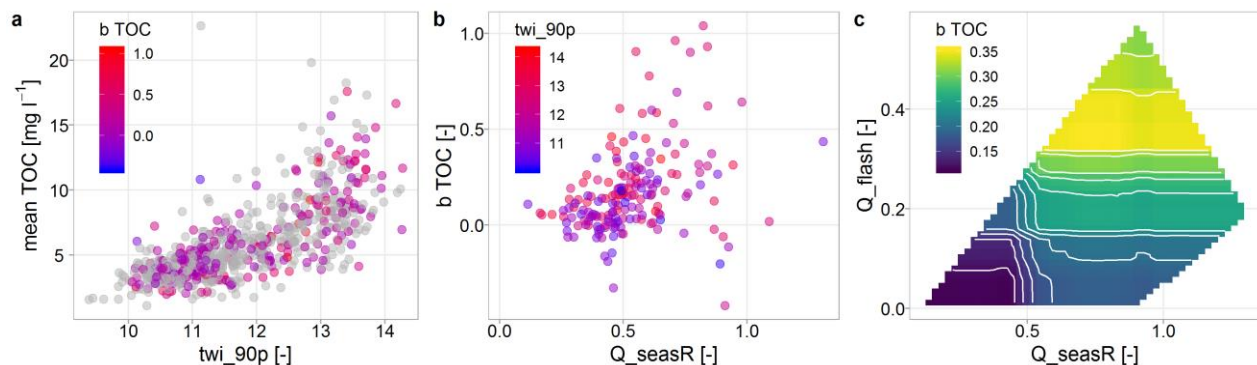


Figure 9. Mean TOC concentrations against twi_90p (a), slope b of TOC against seasonality of Q (Q_{seasR} , see Table S2) with colors according to twi_90p from observations (b), and partial dependence plot of slope b TOC from RF model for the variables seasonality and flashiness of Q (Q_{seasR} , Q_{flash}) (c).

However, even with hydrological descriptors, a substantial part of variability in TOC export dynamics between the studied catchments remains largely unexplained, which may be linked to other drivers of TOC export next to Q, e.g. the temperature (Musolff et al., 2018; Winterdahl et al., 2014). Winterdahl et al. (2014) found DOC-Q correlation coefficients across Sweden to negatively relate to the mean annual temperature, i.e. DOC export becomes more

hydrology driven with lower mean temperatures. This relation could not be observed in our study, possibly, because the mean annual temperatures across our study catchments were generally higher (**Figure 1b**) with an average mean temperature of 8.8°C compared to the maximum mean temperature of 8.6°C in Winterdahl et al. (2014). In this study, we observed that hydrology strongly controls the export only in study catchments with flatter topography: for TOC-Q relationships with $R^2 \geq 0.5$, the topographic slope was $< 2.1^\circ$ and $\text{twi_90p} > 12.2$, while the catchments with lower R^2 had a higher mean topographic slope $= 4.3^\circ$ and lower mean $\text{twi_90p} = 11.7$. Moreover, antecedent conditions, especially riparian soil temperatures and moisture and the occurrence of previous events, are known to control DOC production and shape export patterns in combination with temporally variable hydrological connectivity (Wen et al., 2020; Werner et al., 2019; Winterdahl et al., 2011). Variable antecedent conditions likely cause variable source heterogeneity resulting in export variability that cannot be explained by spatio-temporally aggregated catchment characteristics.

4.2. Are Riparian Wetlands Hot Spots of Interacting Nutrient Cycles Across the Wide Range of Catchments?

Riparian wetlands are potential hot spots of biogeochemical processes due to high hydrologic connectivity to the streams and variable redox conditions during dry and wet cycles with changing water tables (Burt, 2005; McClain et al., 2003). The twi_90p is considered a proxy for the extent of riparian wetlands (Musolff et al., 2018) and was found to be an important predictor for export metrics of the investigated major nutrients, i.e. mean TOC concentrations and slope b of $\text{NO}_3\text{-N}$ and $\text{PO}_4\text{-P}$. Thus we discuss the role of possible nutrient interactions within riparian wetlands.

Catchments with a high twi_90p tend to have high mean TOC and low mean $\text{NO}_3\text{-N}$ concentrations, whereas high $\text{NO}_3\text{-N}$ concentrations were mostly observed in catchments with lower twi_90p and lower mean TOC concentrations (**Figure 10a**). The negative relationship between $\text{NO}_3\text{-N}$ and TOC concentrations could be linked to denitrification under anoxic conditions, the redox reaction with DOC as the electron donor and NO_3 as acceptor, as has been also observed and discussed in several previous studies (e.g., Dupas et al., 2017; Musolff, Selle, et al., 2017; Taylor & Townsend, 2010). Thus riparian wetland denitrification could be part of the increased natural $\text{NO}_3\text{-N}$ attenuation in lowlands (see Section 4.1.1.). Mean TOC were also positively correlated to slope b of $\text{NO}_3\text{-N}$ and both to the twi_90p (see **Figure 10c** and Figure 5). This could indicate that denitrification in riparian wetlands during summer low-flows enhances a positive $\text{NO}_3\text{-Q}$ relationship. This would support the finding that reactivity results in or increases concentration heterogeneity leading to stronger export patterns. However, as the twi_90p is also correlated to het_v ($r=0.75$), which was the dominant control of slope b of $\text{NO}_3\text{-N}$, the additional contribution of this interaction within riparian wetland cannot be fully disentangled here.

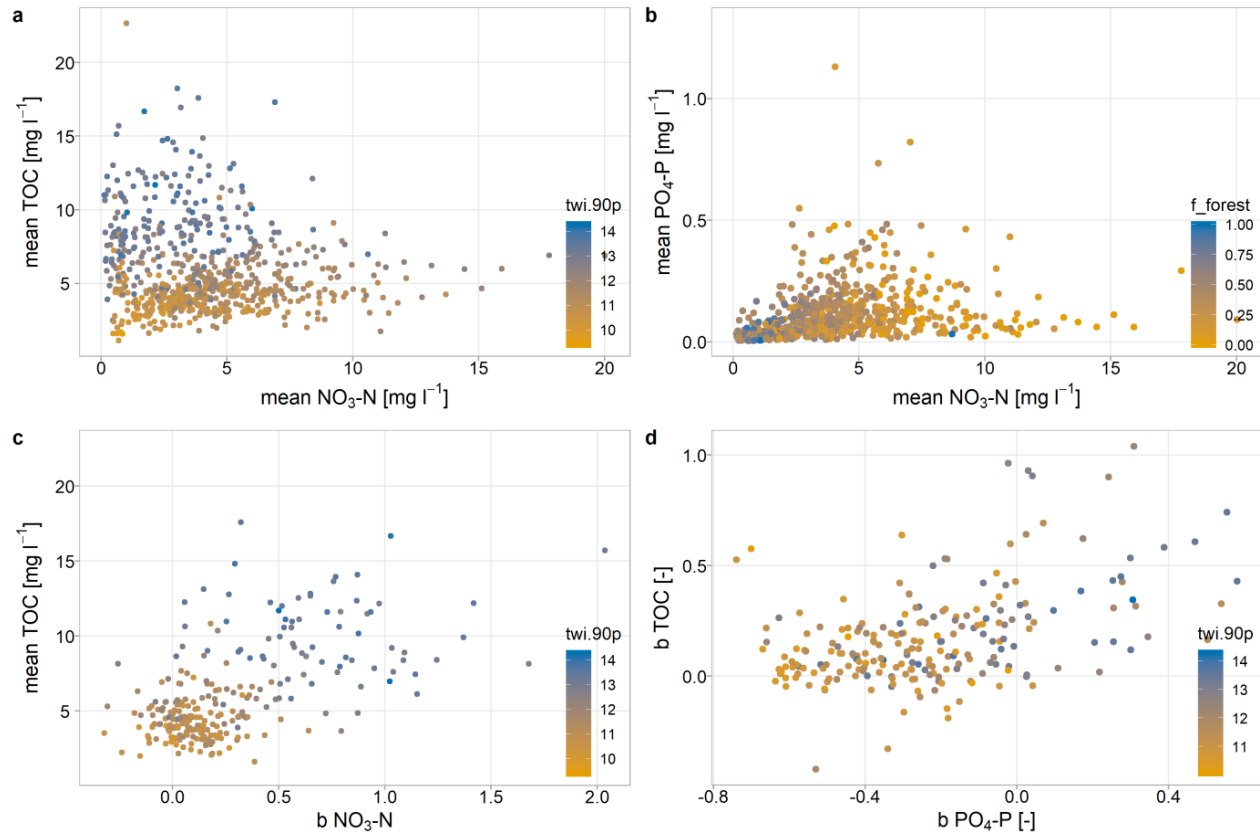


Figure 10. Interaction between metrics of different nutrients in scatterplots, a) mean TOC against mean $\text{NO}_3\text{-N}$ concentrations, b) mean $\text{PO}_4\text{-P}$ against mean $\text{NO}_3\text{-N}$ concentrations, c) mean TOC against $b \text{ NO}_3\text{-N}$ and d) slope of $\text{PO}_4\text{-P}$ against TOC.

Additionally, NO_3 can act as a redox buffer and prevent reductive PO_4 release from riparian wetlands (e.g., Dupas, Gruau, et al., 2015; Gu et al., 2017; Musolff, Selle, et al., 2017), which is expected to cause a negative relation between $\text{NO}_3\text{-N}$ and $\text{PO}_4\text{-P}$ concentrations in catchments with high twi_{90p} . Over the whole range of catchments, the concentrations show a positive relation ($r=0.45$, see **Figure 5** and **Figure 10b**), which is plausible as both nutrients primarily underlie the anthropogenic impact (urban and agricultural, not forest) and could mask interaction in riparian wetlands. However, even in catchments without point sources, this negative relation was not obvious. Though the interaction between $\text{NO}_3\text{-N}$ and $\text{PO}_4\text{-P}$ does not seem to control the variability of temporally aggregated concentrations among catchments, it could be relevant on other scales, e.g. in long-term trends or seasonal patterns.

C-Q slope b of TOC and $\text{PO}_4\text{-P}$ both relate to high twi_{90p} (**Figure 10d**; $r=0.28$ for TOC, $r=0.46$ for $\text{PO}_4\text{-P}$, Figure S4) and correlate positively ($r=0.41$, **Figure 5**). This suggests that both nutrients could be mobilized in riparian wetlands, which could be linked to dissolution under reducing conditions, e.g. due to decreasing NO_3 concentrations as redox buffers, as discussed by Musolff, Selle, et al. (2017).

Over the wide range of studied catchments, nutrient interactions within riparian wetlands possibly affect the variability in catchment responses but they are hard to disentangle from other dominant factors such as attenuation in aquifers and mobilization of diffuse sources. Here, we

suggest to more rigorously test the role of riparian wetlands in a wide set of catchments allowing to group for dominant factors.

4.3. Archetypal Ranges of Nutrient Export

Over the wide range of investigated catchments, solute-specific ranges of the export patterns and regimes were apparent for each nutrient including gradual transitions within the ranges (**Figure 3** and **Figure 11**). Accordingly, about 70% of the catchments classify into the respective dominant groups of each nutrient. Solute-specific prevalence of one pattern and regime has also been reported previously, e.g. by Minaudo et al. (2019) and Moatar et al. (2017), though this consistency might be surprising considering the multitude of processes affecting nutrient cycling, mobilization, transport, and retention. Nevertheless, other studies have also reported export patterns for the non-dominant classes, e.g. Zarnetske et al. (2018) found negative C-Q relationships for DOC in about 20% of the 1006 U.S. catchments and Underwood et al. (2017) found different segmented types of positive and neutral C-Q patterns for dissolved P. Thompson et al. (2011) showed ranges of export regimes for $\text{PO}_4\text{-P}$ and $\text{NO}_3\text{-N}$ which include but also go beyond the respective dominant regime (i.e. chemostatic $\text{PO}_4\text{-P}$ and chemodynamic $\text{NO}_3\text{-N}$ export). Altogether, there is evidence that a substance-specific continuum in patterns and regimes exists which is determined by the bandwidth of solute-specific processes and their variable hierarchies. The properties of the solute or particulate have a major control on processes that lead to mobilization, transport and reactivity and thus export of the nutrient, while the variability within the archetypal ranges is partly linked to catchment characteristics as shown and addressed by PLSR and RF (see Section 3.4).

Dominant controls and characteristics that are linked to the solute-specific ranges have been discussed in the preceding chapters and are synthesized in **Figure 11**. For $\text{NO}_3\text{-N}$, we found a strong interaction between anthropogenic and natural controls: while agricultural inputs define a baseline for mean $\text{NO}_3\text{-N}$ concentrations, natural attenuation creates deviations lowering the mean $\text{NO}_3\text{-N}$. This subsurface denitrification creates vertical concentration heterogeneity resulting in chemodynamic enrichment patterns. For $\text{PO}_4\text{-P}$, natural P cycling strongly interacts with anthropogenic sources both from point sources, which link to mean $\text{PO}_4\text{-P}$ concentrations, and diffuse sources, which link to positive C-Q slopes. For TOC, interaction between anthropogenic and natural controls was not apparent, as the topography strongly controlled mean concentrations and the spatial variability of export dynamics was partly explained by hydrological variability. **Figure 11** summarizes these dominating characteristics within specific parts of the observed ranges.

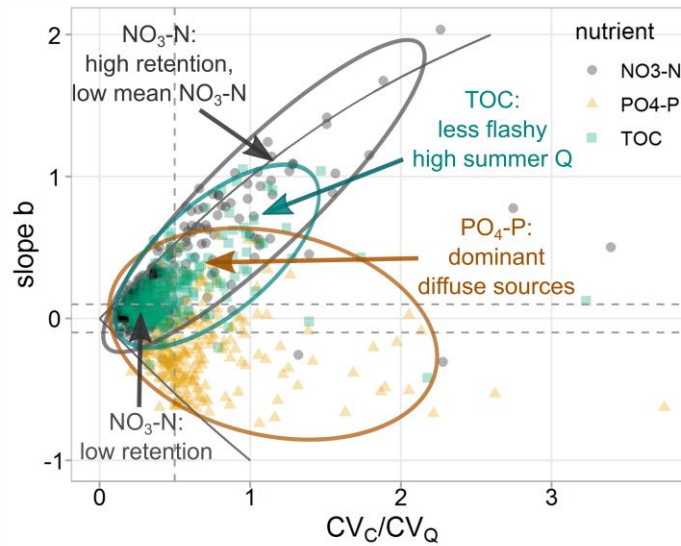


Figure 11. Archetypal ranges of solute-specific export patterns and regimes with examples of typical characteristics of catchments in this area of the nutrient-specific range indicated by arrows. Colors of points, ellipse, arrows and typical characteristics are according to the nutrient (black - $\text{NO}_3\text{-N}$, orange - $\text{PO}_4\text{-P}$, green - TOC).

4.4. Limitations

The investigation of mean concentrations, export patterns and regimes and the subsequent identification of predictors underlie the assumption of stationarity of catchment-functioning over the analysed time period. Even if this is not true in some catchments for some nutrients, aggregating over this relatively short period (here 2000-2015) should be acceptable and not corrupt the results of the general behaviour we interpreted.

Our analysis aggregates low-frequency data over different seasons and climatic conditions assuming that general relationships remain apparent and interpretable. Several studies have chosen other approaches differentiating low-flow and high-flow conditions by generally dividing the C-Q relationships (Moatar et al., 2017; Underwood et al., 2017) or by distinguishing event and base flow conditions (Minaudo et al., 2019). Burns et al. (2019) and Duncan et al. (2017) discuss that interannual aggregation may lead to more chemostatic C-Q relationships and high-frequency sampling may reveal contrasting patterns and processes. Generally, ambivalent relationships between C and Q can cause dispersion in C-Q regressions (Bol et al., 2018). We acknowledge that our approach could thus enhance scatter in the C-Q relationships and miss subscale processes, but the analysis still allowed us to observe spatial and solute-specific patterns and interpret the overarching control of catchment characteristics.

Further, the spatial aggregation of characteristics over the complete catchments may mask drivers at smaller scale. This might be even wanted to reveal hierarchies of processes at catchment scale, but if various small-scale processes dominate the response at catchment scale, this could also be a reason for a part of the variability in C-Q metrics not explained, as we saw for example for $\text{PO}_4\text{-P}$.

Here, we note as well that ambiguity in certain predictors can limit clear linking of the identified dominant controls to drivers and processes. We tried to reduce this uncertainty by

using two composite approaches as model ensemble which allowed us to better discuss generalities in the dependencies between descriptors and responses, as recommended by (Schmidt et al., 2020).

The cross-validation quantifies the model uncertainty which partly relates to tendencies of overfitting but also to the subset and variability of samples. The model uncertainty can be interpreted based on the standard deviation of cross-validated model performances given in **Figure 6** and on comparisons to model performances of supplemental models with smaller sample sizes (Table S4-5, S8-10). The uncertainty varies largely between models: the standard deviations of R^2_{CrossVal} were lowest for mean $\text{NO}_3\text{-N}$ and mean TOC concentrations with 7.3-9.6% and highest for slope b of TOC in RF with 19.0% (**Figure 6**). The uncertainties are mostly similar for corresponding PLSR and RF models, though there is a slight tendency for higher uncertainty in RF models which indicates that RF models could overfit more easily to the train data. With this they also tend to reach slightly higher performances in cross-validation relating to the higher flexibility of the model. Therefore, we would like to generally promote that final model performances should not be judged without considering the model uncertainty in relation to the set of samples, as the predictability could be easily overestimated. This general variability also explains small deviations in variable rankings when using a different subset of samples, especially when descriptors have a similar variable importance.

5 Conclusions

To infer drivers of nutrient export over a wide range of catchments, we classified 278 independent catchments across Germany based on C-Q relationships and linked them to catchment characteristics using PLSR and RF models, while for mean concentrations we used in total 787 independent catchments.

We identified nutrient specific ranges in C-Q relationships with about 70% of catchments classifying into the respective dominant C-Q patterns and regimes. Enrichment patterns and chemostatic regimes prevailed for $\text{NO}_3\text{-N}$ and TOC export, whereas dilution and chemodynamic export prevailed for $\text{PO}_4\text{-P}$. The archetypal ranges of export dynamics demonstrate a solute-specific prevalence and possible range of hierarchies among processes. The variability within the ranges could partly be explained by distinct anthropogenic and natural catchment characteristics though catchments remain complex systems and certain variability remained unexplained.

For $\text{NO}_3\text{-N}$, we found that natural attenuation potentially buffers anthropogenic inputs reducing mean $\text{NO}_3\text{-N}$ concentrations and creating concentration heterogeneity within the catchment that controls export dynamics. Attenuation was found most dominant in lowland areas with deep sedimentary aquifers. According to the observed relationship, enrichment patterns in agricultural areas could indicate effective subsurface reactivity. On the other hand, chemostasis links to low subsurface attenuation and concentration homogeneity. This means there is a strong interaction of anthropogenic and natural drivers, though the latter is not ubiquitous and possibly not permanent.

Diffuse and point sources were found relevant for riverine $\text{PO}_4\text{-P}$ concentrations even if the variability in metrics was hard to predict by catchment characteristics. Mean $\text{PO}_4\text{-P}$ were linked to point sources though not strongly, while the variability in $\text{PO}_4\text{-P}$ dynamics was better explained by diffuse sources. Probably, P cycling reshapes $\text{PO}_4\text{-P}$ responses in the streams decoupling them to some degree from their source configuration and land-stream transfer

processes. Stronger P cycling during low-flow could explain that dilution patterns prevail but are widely unrelated to point sources, while the fewer enrichment patterns could be linked to diffuse sources and P saturation in the top soils. Anthropogenic drivers, including point sources and P soil status, proved to be dominant, but responses are strongly reshaped by natural drivers hampering predictions at catchment scale.

Natural topographic settings dominantly controlled TOC concentrations: mean TOC were strongly linked to the abundance of riparian wetlands as source areas. The hydrological descriptors, especially relatively higher summer discharges, increased the explained variability of export metrics though the unexplained part remained relatively high suggesting other relevant time-variant controls such as antecedent conditions and temperature. At the same time, temporally variable conditions and interacting processes can cause dispersion and ambiguity in aggregated C-Q relationships and thus reduce overall predictability. We could not find a strong influence of anthropogenic sources and drivers for mean TOC concentrations and TOC exports.

Altogether, we found our hypothesis that source heterogeneity widely controls export dynamics partly approved. For $\text{NO}_3\text{-N}$, not source but vertical concentration heterogeneity widely controlled export dynamics, which likely results from subsurface reactivity as the dominant process. Strong enrichment patterns occurred in areas with high attenuation, whereas without subsurface reactivity and concentration homogeneity, chemostatic export prevailed. For $\text{PO}_4\text{-P}$, the strength of diffuse sources was dominant suggesting that heterogeneity in P soil status between top soil and deeper layers drives export patterns. As TOC export patterns remained largely unexplained by aggregated characteristics, variable source strength and heterogeneity causing intra-annual changes in the C-Q relationships could be the reason. For both $\text{PO}_4\text{-P}$ and TOC, directly hydrologically connected areas are prerequisite for translating vertical source heterogeneity to chemodynamic export due to their strong sorption tendency. This connectivity can be provided by drained areas creating preferential flow paths or given for locations close to the stream such as riparian zones.

As some of the identified controls, especially the anthropogenic, have developed over time, the catchment responses may also follow trends on long term. For $\text{PO}_4\text{-P}$, for example, reductions in point sources and increasing P legacies in agricultural soils might have led to the visibility of enrichment patterns by shifting the dominance of processes. $\text{NO}_3\text{-N}$ could follow trajectories from more chemodynamic to more chemostatic export if subsurface reactivity decreased over time. With rising temperatures and heavier storm events due to climate change (EEA, 2019), nutrient export might change as well as biogeochemical interactions linked to temperatures and redox conditions. For example, TOC exports might increase with prolonged production times and more variable hydrological connectivity, potentially also enhanced by lower NO_3 redox buffers when depositions and concentrations decrease (Clark et al., 2010). This would mean an indirect anthropogenic impact on TOC due to nutrient interactions.

Our findings can support water quality management by giving orientation on how or in what range catchments with certain characteristics are expected to respond. If chemostatic $\text{NO}_3\text{-N}$ export is apparent, missing or exhausting denitrification capacity of the system might be the reason and, in consequence, more efforts for mitigation measures and reduced inputs to protect the water quality might be required. Nevertheless, in systems with apparent effective attenuation and chemodynamic $\text{NO}_3\text{-N}$ export, the exported loads might still be high, the natural buffer might exhaust in the future or the decrease in concentration be linked to strongly unbalanced systems with enormous recovery times. Therefore, controlling inputs seems vital in both cases.

For $\text{PO}_4\text{-P}$, we found that the contribution of diffuse sources can be dominant which indicates that focussing on point sources for P management is not up-to-date, especially because diffuse source mobilization can result in high exported loads affecting downstream water bodies. Water quality modelers can benefit from the presented solute-specific ranges of export dynamics and the identified dominant controls, e.g. the effective reactivity which impacts both concentrations and dynamics of $\text{NO}_3\text{-N}$ and biogeochemical processes relating to P cycling.

Author Contributions

PE conducted the main data preprocessing and analysis, prepared visualizations of results and wrote the manuscript. AM designed and supervised the study. AM, RK, MW, PE mainly set up the data base of water quantity and quality and geoinformation of catchments, the data management, and quality checks. LK calculated vertical heterogeneity across Germany. All authors contributed to writing the manuscript.

Acknowledgments and Data

We thank the Federal authorities for providing water sample data and all contributors to setting up the used data base, including Thomas Grau, Teresa Nitz and Joni Dehaspe. We thank Martin Bach and Uwe Häußermann for providing the N surplus data. We thank Soohyun Yang and Olaf Büttner for providing the data of small water treatment plants in Germany. We acknowledge the E-OBS dataset from the EU-FP6 project UERRA (<http://www.uerra.eu>) and the Copernicus Climate Change Service, and the data providers in the ECA&D project (<https://eca.knmi.nl>). We further acknowledge several organizations for providing data products used in this study, including the BfG, BGR, SGD, EEA, FAO, IIASA, ISRIC, ISSCAS and JRC. The authors thank for the funding by the Initiative and Networking Fund of the Helmholtz Association through the project Advanced Earth System Modelling Capacity (ESM) (www.esm-project.net). The authors declare no conflict of interest.

Datasets for this research are available in these in-text data citation references: Ebeling (2020b) [the repository will be published at acceptance, for revision it is already discoverable], Ebeling (2020a) [published at acceptance, for revision discoverable], Musolff et al. (2020) [original data in institutional repository] and Musolff (2020). Further original datasets used for this research are referenced in **Table 1** and in the text.

References

- Ameli, A. A., Beven, K., Erlandsson, M., Creed, I. F., McDonnell, J. J., & Bishop, K. (2017). Primary weathering rates, water transit times, and concentration-discharge relations: A theoretical analysis for the critical zone. *Water Resources Research*, 53(1), 942-960. <https://agupubs.onlinelibrary.wiley.com/doi/abs/10.1002/2016WR019448>
- Bach, M., Klement, L., & Häußermann, U. (2016). *Bewertung von Maßnahmen zur Verminderung von Nitrateinträgen in die Gewässer auf Basis regionalisierter Stickstoff Überschüsse. Teil I: Beitrag zur Entwicklung einer ressortübergreifenden Stickstoffstrategie Zwischenbericht*. Retrieved from Dessau-Roßlau:
- Ballabio, C., Lugato, E., Fernández-Ugalde, O., Orgiazzi, A., Jones, A., Borrelli, P., et al. (2019). Mapping LUCAS topsoil chemical properties at European scale using Gaussian process regression. *Geoderma*, 355, 113912. <http://www.sciencedirect.com/science/article/pii/S0016706119304768>
- Basu, N. B., Destouni, G., Jawitz, J. W., Thompson, S. E., Loukinova, N. V., Darracq, A., et al. (2010). Nutrient loads exported from managed catchments reveal emergent biogeochemical stationarity. *Geophysical Research Letters*, 37(23). <https://agupubs.onlinelibrary.wiley.com/doi/full/10.1029/2010GL045168>

- Basu, N. B., Thompson, S. E., & Rao, P. S. C. (2011). Hydrologic and biogeochemical functioning of intensively managed catchments: A synthesis of top-down analyses. *Water Resources Research*, 47. <Go to ISI>://WOS:000296340500002
- Battin, T. J., Kaplan, L. A., Findlay, S., Hopkinson, C. S., Marti, E., Packman, A. I., et al. (2008). Biophysical controls on organic carbon fluxes in fluvial networks. *Nature Geoscience*, 1(2), 95-100. Article. <Go to ISI>://WOS:000256433300011
- Behrendt, H. (1999). *Nährstoffbilanzierung der Flussgebiete in Deutschland*. Retrieved from
- Benettin, P., Bailey, S. W., Rinaldo, A., Likens, G. E., McGuire, K. J., & Botter, G. (2017). Young runoff fractions control streamwater age and solute concentration dynamics. *Hydrological Processes*, 31(16), 2982-2986. <https://onlinelibrary.wiley.com/doi/abs/10.1002/hyp.11243>
- Beven, K. J., & Kirkby, M. J. (1979). A physically based, variable contributing area model of basin hydrology / Un modèle à base physique de zone d'appel variable de l'hydrologie du bassin versant. *Hydrological Sciences Bulletin*, 24(1), 43-69.
- Verordnung über Höchstmengen für Phosphate in Wasch-und Reinigungsmitteln vom 4.6.1980: PHöchstMengV; 1980, (1980).
- BGR. (2003). *Mean Annual Rate of Percolation from the Soil in Germany (SWR1000)*, *Hydrogeologischer Atlas von Deutschland*. Retrieved from: https://www.bgr.bund.de/DE/Themen/Boden/Bilder/Bod_Themenkarten_HAD_4-5_g.html
- BGR. (2018). *Bodenübersichtskarte der Bundesrepublik Deutschland 1:250.000 (BUEK250)*. Soil map of Germany 1:250,000. Retrieved from: <https://produktcenter.bgr.de/terraCatalog/Start.do>
- BGR & SGD. (2015). *Hydrogeologische Raumgliederung von Deutschland (HYRAUM)*. Retrieved from: https://www.bgr.bund.de/DE/Themen/Wasser/Projekte/abgeschlossen/Beratung/Hyraum/hyraum_projektbeschr.html?nn=1557832
- BGR & UNESCO (eds.). (2014). *International Hydrogeological Map of Europe 1 : 1,500,000 (IHME1500)*. Digital map data v1.1. Retrieved from: <http://www.bgr.bund.de/ihme1500/>
- Bieroza, M. Z., & Heathwaite, A. L. (2015). Seasonal variation in phosphorus concentration–discharge hysteresis inferred from high-frequency in situ monitoring. *Journal of Hydrology*, 524, 333-347.
- Bishop, K., Seibert, J., Köhler, S., & Laudon, H. (2004). Resolving the Double Paradox of rapidly mobilized old water with highly variable responses in runoff chemistry. *Hydrological Processes*, 18(1), 185-189. <https://onlinelibrary.wiley.com/doi/abs/10.1002/hyp.5209>
- BMU. (2000). *Hydrologischer Atlas von Deutschland* (N. u. R. Bundesministerium Für Umwelt Ed.). Bonn/Berlin: Datenquelle: Hydrologischer Atlas von Deutschland/BfG, 2000.
- Bol, R., Gruau, G., Mellander, P.-E., Dupas, R., Bechmann, M., Skarbøvik, E., et al. (2018). Challenges of Reducing Phosphorus Based Water Eutrophication in the Agricultural Landscapes of Northwest Europe. *Frontiers in Marine Science*, 5(276). Review. <https://www.frontiersin.org/article/10.3389/fmars.2018.00276>
- Botter, G., Basso, S., Rodriguez-Iturbe, I., & Rinaldo, A. (2013). Resilience of river flow regimes. *Proc Natl Acad Sci U S A*, 110(32), 12925-12930. <https://www.ncbi.nlm.nih.gov/pubmed/23878257>
- Bouraoui, F., & Grizzetti, B. (2011). Long term change of nutrient concentrations of rivers discharging in European seas. *Science of The Total Environment*, 409(23), 4899-4916. <http://www.sciencedirect.com/science/article/pii/S0048969711008394>
- Bouwman, A. F., Bierkens, M. F. P., Griffioen, J., Hefting, M. M., Middelburg, J. J., Middelkoop, H., & Slomp, C. P. (2013). Nutrient dynamics, transfer and retention along the aquatic continuum from land to ocean: towards integration of ecological and biogeochemical models. *Biogeosciences*, 10(1), 1-22. <https://www.biogeosciences.net/10/1/2013/>
- Breiman, L. (2001). Random Forests. *Machine Learning*, 45(1), 5-32. journal article. <https://doi.org/10.1023/A:1010933404324>
- Bricker, S. B., Clement, C. G., Pirhalla, D. E., Orlando, S. P., & Farrow, D. R. G. (1999). *National Estuarine Eutrophication Assessment: Effects of Nutrient Enrichment in the Nation's Estuaries*. Retrieved from Silver Spring, MD: https://ian.umces.edu/nea/pdfs/eutro_report.pdf
- Burns, D. A., Pellerin, B. A., Miller, M. P., Capel, P. D., Tesoriero, A. J., & Duncan, J. M. (2019). Monitoring the riverine pulse: Applying high-frequency nitrate data to advance integrative understanding of biogeochemical and hydrological processes. *WIREs Water*, 6(4), e1348. <https://onlinelibrary.wiley.com/doi/abs/10.1002/wat2.1348>
- Burt, T. P. (2005). A third paradox in catchment hydrology and biogeochemistry: decoupling in the riparian zone. *Hydrological Processes*, 19(10), 2087-2089. <https://onlinelibrary.wiley.com/doi/abs/10.1002/hyp.5904>

- Büttner, O. (2020a). *DE-WWTP - data collection of wastewater treatment plants of Germany (status 2015, metadata)*, HydroShare. Retrieved from: <https://doi.org/10.4211/hs.712c1df62aca4ef29688242eeab7940c>
- Büttner, O. (2020b). The waste water treatment data collection for Germany 2015 (DE-WWTP). <https://www.ufz.de/record/dmp/archive/7800>
- Center for International Earth Science Information Network - CIESIN - Columbia University. (2017). *Gridded Population of the World, Version 4 (GPWv4): Population Density, Revision 10*. Retrieved from: <https://doi.org/10.7927/H4DZ068D>
- Clark, J. M., Bottrell, S. H., Evans, C. D., Monteith, D. T., Bartlett, R., Rose, R., et al. (2010). The importance of the relationship between scale and process in understanding long-term DOC dynamics. *Science of The Total Environment*, 408(13), 2768-2775. <http://www.sciencedirect.com/science/article/pii/S0048969710002160>
- CLC. (2016). *CORINE Land Cover 2012 v18.5*. Retrieved from: <https://land.copernicus.eu/pan-european/corine-land-cover>
- Copeland, C. (2016). Clean Water Act: A Summary of the Law [Press release]
- Cornes, R. C., van der Schrier, G., van den Besselaar, E. J. M., & Jones, P. D. (2018). An Ensemble Version of the E-OBS Temperature and Precipitation Data Sets. *Journal of Geophysical Research: Atmospheres*, 123(17), 9391-9409. <https://agupubs.onlinelibrary.wiley.com/doi/abs/10.1029/2017JD028200>
- Damania, R., Desbureaux, S., Rodella, A.-S., Russ, J. D., & Zaveri, E. D. (2019). *Quality Unknown : The Invisible Water Crisis* (Report No 140973). Retrieved from
- De Jager, A., & Vogt, J. (2007). *Rivers and Catchments of Europe - Catchment Characterisation Model (CCM)*. Retrieved from: <http://data.europa.eu/89h/fe1878e8-7541-4c66-8453-afdae7469221>
- Duncan, J. M., Welty, C., Kemper, J. T., Groffman, P. M., & Band, L. E. (2017). Dynamics of nitrate concentration-discharge patterns in an urban watershed. *Water Resources Research*, 53(8), 7349-7365. <https://agupubs.onlinelibrary.wiley.com/doi/abs/10.1002/2017WR020500>
- Dupas, R., Delmas, M., Dorioz, J.-M., Garnier, J., Moatar, F., & Gascuel-Oudou, C. (2015). Assessing the impact of agricultural pressures on N and P loads and eutrophication risk. *Ecological Indicators*, 48, 396-407.
- Dupas, R., Gascuel-Oudou, C., Gilliet, N., Grimaldi, C., & Gruau, G. (2015). Distinct export dynamics for dissolved and particulate phosphorus reveal independent transport mechanisms in an arable headwater catchment. *Hydrological Processes*, 29(14), 3162-3178. <https://onlinelibrary.wiley.com/doi/abs/10.1002/hyp.10432>
- Dupas, R., Gruau, G., Gu, S., Humbert, G., Jaffrézic, A., & Gascuel-Oudou, C. (2015). Groundwater control of biogeochemical processes causing phosphorus release from riparian wetlands. *Water Research*, 84, 307-314. <http://www.sciencedirect.com/science/article/pii/S0043135415301500>
- Dupas, R., Jomaa, S., Musolff, A., Borchardt, D., & Rode, M. (2016). Disentangling the influence of hydroclimatic patterns and agricultural management on river nitrate dynamics from sub-hourly to decadal time scales. *Science of The Total Environment*, 571, 791-800. <http://www.sciencedirect.com/science/article/pii/S004896971631498X>
- Dupas, R., Musolff, A., Jawitz, J. W., Rao, P. S. C., Jäger, C. G., Fleckenstein, J. H., et al. (2017). Carbon and nutrient export regimes from headwater catchments to downstream reaches. *Biogeosciences*, 14(18), 4391-4407. <https://www.biogeosciences.net/14/4391/2017/>
- Dupas, R., Tittel, J., Jordan, P., Musolff, A., & Rode, M. (2018). Non-domestic phosphorus release in rivers during low-flow: Mechanisms and implications for sources identification. *Journal of Hydrology*, 560, 141-149.
- Ebeling, P. (2020a). *CCDB - catchment characteristics data base Germany*, HydroShare. Retrieved from: <http://www.hydroshare.org/resource/0fc1b5b1be4a475aacfd9545e72e6839>
- Ebeling, P. (2020b). *WQQDB - water quality metrics for catchments across Germany*, HydroShare. Retrieved from: <http://www.hydroshare.org/resource/9b4deeca259b4f7398ce72121b4e2979>
- COUNCIL DIRECTIVE of 21 May 1991 concerning urban waste water treatment (91/271/EEC), (1991).
- EEA. (2013). *DEM over Europe from the GMES RDA project (EU-DEM, resolution 25m) - version 1, Oct. 2013*.
- EEA. (2016). *EU-Hydro River Network* [geodata]. Retrieved from: <https://land.copernicus.eu/imagery-in-situ/eu-hydro/eu-hydro-public-beta/eu-hydro-river-network>
- EEA. (2018). *European waters. Assessment of status and pressures 2018* (EEA Report No 7/201). Retrieved from <https://www.eea.europa.eu/publications/state-of-water>
- EEA. (2019). *The European environment — state and outlook 2020* (ISBN 978-92-9480-090-9). Retrieved from <https://www.eea.europa.eu/publications/soer-2020>
- Council Directive 91/676/EEC of 12 December 1991 concerning the protection of waters against pollution caused by nitrates from agricultural sources, (1991).

- EEC. (2000). Directive 2000/60/EC of the European Parliament and of the Council of 23 October 2000 establishing a framework for Community action in the field of water policy. *Official Journal of the European Communities*, L 327, 1 - 73.
- Ehrhardt, S., Kumar, R., Fleckenstein, J. H., Attinger, S., & Musolff, A. (2019). Trajectories of nitrate input and output in three nested catchments along a land use gradient. *Hydrol. Earth Syst. Sci.*, 23(9), 3503-3524. <https://www.hydrol-earth-syst-sci.net/23/3503/2019/>
- EPA. (2017). *National Water Quality Inventory: Report to Congress*. Retrieved from https://www.epa.gov/sites/production/files/2017-12/documents/305brtc_finalowow_08302017.pdf
- Evans, D. M., Schoenholtz, S. H., Wigington, P. J., Griffith, S. M., & Floyd, W. C. (2014). Spatial and temporal patterns of dissolved nitrogen and phosphorus in surface waters of a multi-land use basin. *Environmental Monitoring and Assessment*, 186(2), 873-887. <https://doi.org/10.1007/s10661-013-3428-4>
- FAO/IIASA/ISRIC/ISSCAS/JRC. (2012). *Harmonized World Soil Database (version 1.2)*. Retrieved from: <https://webarchive.iiasa.ac.at/Research/LUC/External-World-soil-database/HTML/>
- Fischer, P., Pöthig, R., & Venohr, M. (2017). The degree of phosphorus saturation of agricultural soils in Germany: Current and future risk of diffuse P loss and implications for soil P management in Europe. *Science of The Total Environment*, 599-600, 1130-1139. <http://www.sciencedirect.com/science/article/pii/S0048969717306629>
- Gentry, L. E., David, M. B., Royer, T. V., Mitchell, C. A., & Starks, K. M. (2007). Phosphorus Transport Pathways to Streams in Tile-Drained Agricultural Watersheds. *Journal of Environmental Quality*, 36(2), 408-415. <http://dx.doi.org/10.2134/jeq2006.0098>
- Godsey, S. E., Kirchner, J. W., & Clow, D. W. (2009). Concentration-discharge relationships reflect chemostatic characteristics of US catchments. *Hydrological Processes*, 23(13), 1844-1864.
- Gomez-Velez, J. D., Harvey, J. W., Cardenas, M. B., & Kiel, B. (2015). Denitrification in the Mississippi River network controlled by flow through river bedforms. *Nature Geoscience*, 8, 941. <https://doi.org/10.1038/ngeo2567>
- Gruber, N., & Galloway, J. N. (2008). An Earth-system perspective of the global nitrogen cycle. *Nature*, 451, 293. <https://doi.org/10.1038/nature06592>
- Gu, S., Gruau, G., Dupas, R., Rumpel, C., Creme, A., Fovet, O., et al. (2017). Release of dissolved phosphorus from riparian wetlands: Evidence for complex interactions among hydroclimate variability, topography and soil properties. *Sci Total Environ*, 598, 421-431. <https://www.ncbi.nlm.nih.gov/pubmed/28448934>
- Gupta, H. V., Perrin, C., Blöschl, G., Montanari, A., Kumar, R., Clark, M., & Andréassian, V. (2014). Large-sample hydrology: a need to balance depth with breadth. *Hydrol. Earth Syst. Sci.*, 18(2), 463-477. <https://www.hydrol-earth-syst-sci.net/18/463/2014/>
- Hahn, C., Prasuhn, V., Stamm, C., & Schulin, R. (2012). Phosphorus losses in runoff from manured grassland of different soil P status at two rainfall intensities. *Agriculture, Ecosystems & Environment*, 153, 65-74. <http://www.sciencedirect.com/science/article/pii/S0167880912001004>
- Hannappel, S., Köpp, C., & Bach, T. (2018). Charakterisierung des Nitratabbauvermögens der Grundwasserleiter in Sachsen-Anhalt. *Grundwasser*, 23(4), 311-321. journal article. <https://doi.org/10.1007/s00767-018-0402-7>
- Hansen, A. T., Dolph, C. L., Foufoula-Georgiou, E., & Finlay, J. C. (2018). Contribution of wetlands to nitrate removal at the watershed scale. *Nature Geoscience*, 11(2), 127-132. <https://doi.org/10.1038/s41561-017-0056-6>
- Häußermann, U., Bach, M., Klement, L., & Breuer, L. (2019). *Stickstoff-Flächenbilanzen für Deutschland mit Regionalgliederung Bundesländer und Kreise – Jahre 1995 bis 2017. Methodik, Ergebnisse und Minderungsmaßnahmen*. Retrieved from
- Herndon, E. M., Dere, A. L., Sullivan, P. L., Norris, D., Reynolds, B., & Brantley, S. L. (2015). Landscape heterogeneity drives contrasting concentration–discharge relationships in shale headwater catchments. *Hydrol. Earth Syst. Sci.*, 19(8), 3333-3347. <https://www.hydrol-earth-syst-sci.net/19/3333/2015/>
- Howden, N. J. K., Burt, T. P., Worrall, F., Whelan, M. J., & Bieroza, M. Z. (2010). Nitrate concentrations and fluxes in the River Thames over 140 years (1868–2008): are increases irreversible? *Hydrological Processes*, 24(18), 2657-2662. <https://onlinelibrary.wiley.com/doi/abs/10.1002/hyp.7835>
- Hunsaker, C. T., & Johnson, D. W. (2017). Concentration-discharge relationships in headwater streams of the Sierra Nevada, California. *Water Resources Research*, 53(9), 7869-7884.
- Jarvie, H. P., Sharpley, A. N., Withers, P. J. A., Scott, J. T., Haggard, B. E., & Neal, C. (2013). Phosphorus Mitigation to Control River Eutrophication: Murky Waters, Inconvenient Truths, and “Postnormal” Science. *Journal of Environmental Quality*, 42(2), 295-304. <https://access.onlinelibrary.wiley.com/doi/abs/10.2134/jeq2012.0085>

- Jordan, P., Menary, W., Daly, K., Kiely, G., Morgan, G., Byrne, P., & Moles, R. (2005). Patterns and processes of phosphorus transfer from Irish grassland soils to rivers—integration of laboratory and catchment studies. *Journal of Hydrology*, 304(1), 20-34.
<http://www.sciencedirect.com/science/article/pii/S0022169404004731>
- Kalbitz, K., Solinger, S., Park, J.-H., Michalzik, B., & Matzner, E. (2000). CONTROLS ON THE DYNAMICS OF DISSOLVED ORGANIC MATTER IN SOILS: A REVIEW. *Soil Science*, 165(4), 277-304.
https://journals.lww.com/soilsci/Fulltext/2000/04000/CONTROLS_ON_THE_DYNAMICS_OF_DISSOLVED_ORGANIC.1.aspx
- Knoll, L., Breuer, L., & Bach, M. (2019). Large scale prediction of groundwater nitrate concentrations from spatial data using machine learning. *Science of The Total Environment*, 668, 1317-1327.
<http://www.sciencedirect.com/science/article/pii/S004896971931023X>
- Knoll, L., Breuer, L., & Bach, M. (2020). Nation-wide estimation of groundwater redox conditions and nitrate concentrations through machine learning. *Environmental Research Letters*, 15(6), 064004.
<http://dx.doi.org/10.1088/1748-9326/ab7d5c>
- Kunkel, R., Bach, M., Behrendt, H., & Wendland, F. (2004). Groundwater-borne nitrate intakes into surface waters in Germany. *Water Science and Technology*, 49(3), 11-19. <https://doi.org/10.2166/wst.2004.0152>
- Kunkel, R., Herrmann, F., Kape, H.-E., Keller, L., Koch, F., Tetzlaff, B., & Wendland, F. (2017). Simulation of terrestrial nitrogen fluxes in Mecklenburg-Vorpommern and scenario analyses how to reach N-quality targets for groundwater and the coastal waters. *Environmental Earth Sciences*, 76(4), 146.
<https://doi.org/10.1007/s12665-017-6437-8>
- Laudon, H., Berggren, M., Ågren, A., Buffam, I., Bishop, K., Grabs, T., et al. (2011). Patterns and Dynamics of Dissolved Organic Carbon (DOC) in Boreal Streams: The Role of Processes, Connectivity, and Scaling. *Ecosystems*, 14(6), 880-893. journal article. <https://doi.org/10.1007/s10021-011-9452-8>
- Le Moal, M., Gascuel-Oudou, C., Ménesguen, A., Souchon, Y., Étrillard, C., Levain, A., et al. (2019). Eutrophication: A new wine in an old bottle? *Science of The Total Environment*, 651, 1-11.
<http://www.sciencedirect.com/science/article/pii/S0048969718335836>
- Livneh, B., Kumar, R., & Samaniego, L. (2015). Influence of soil textural properties on hydrologic fluxes in the Mississippi river basin. *Hydrological Processes*, 29(21), 4638-4655.
<https://onlinelibrary.wiley.com/doi/abs/10.1002/hyp.10601>
- Lutz, S. R., Trauth, N., Musolff, A., Van Breukelen, B. M., Knöller, K., & Fleckenstein, J. H. (2020). How Important is Denitrification in Riparian Zones? Combining End-Member Mixing and Isotope Modeling to Quantify Nitrate Removal from Riparian Groundwater. *Water Resources Research*, 56(1), e2019WR025528. <https://agupubs.onlinelibrary.wiley.com/doi/abs/10.1029/2019WR025528>
- McClain, M. E., Boyer, E. W., Dent, C. L., Gergel, S. E., Grimm, N. B., Groffman, P. M., et al. (2003). Biogeochemical Hot Spots and Hot Moments at the Interface of Terrestrial and Aquatic Ecosystems. *Ecosystems*, 6(4), 301-312. journal article. <https://doi.org/10.1007/s10021-003-0161-9>
- Meals, D. W., Dressing, S. A., & Davenport, T. E. (2010). Lag Time in Water Quality Response to Best Management Practices: A Review. *Journal of Environmental Quality*, 39(1), 85-96.
<http://dx.doi.org/10.2134/jeq2009.0108>
- Merz, C., Steidl, J., & Dannowski, R. (2009). Parameterization and regionalization of redox based denitrification for GIS-embedded nitrate transport modeling in Pleistocene aquifer systems. *Environmental Geology*, 58(7), 1587. <https://doi.org/10.1007/s00254-008-1665-6>
- Minaudo, C., Dupas, R., Gascuel-Oudou, C., Roubeix, V., Danis, P.-A., & Moatar, F. (2019). Seasonal and event-based concentration-discharge relationships to identify catchment controls on nutrient export regimes. *Advances in Water Resources*, 131, 103379.
<http://www.sciencedirect.com/science/article/pii/S030917081830616X>
- Moatar, F., Abbott, B. W., Minaudo, C., Curie, F., & Pinay, G. (2017). Elemental properties, hydrology, and biology interact to shape concentration-discharge curves for carbon, nutrients, sediment, and major ions. *Water Resources Research*, 53(2), 1270-1287.
- Moatar, F., Floury, M., Gold, A. J., Meybeck, M., Renard, B., Ferréol, M., et al. (2020). Stream Solutes and Particulates Export Regimes: A New Framework to Optimize Their Monitoring. *Frontiers in Ecology and Evolution*, 7(516). Original Research. <https://www.frontiersin.org/article/10.3389/fevo.2019.00516>
- Møller, A. B., Beucher, A., Iversen, B. V., & Greve, M. H. (2018). Predicting artificially drained areas by means of a selective model ensemble. *Geoderma*, 320, 30-42.
<http://www.sciencedirect.com/science/article/pii/S0016706117318116>

- Musolff, A. (2020). *WQADB - water quality and quantity data base Germany: metadata*, HydroShare. Retrieved from: <https://doi.org/10.4211/hs.a42adcbd59a466a9aa56472dfef8721>
- Musolff, A., Fleckenstein, J. H., Opitz, M., Büttner, O., Kumar, R., & Tittel, J. (2018). Spatio-temporal controls of dissolved organic carbon stream water concentrations. *Journal of Hydrology*, 566, 205-215. <http://www.sciencedirect.com/science/article/pii/S0022169418306978>
- Musolff, A., Fleckenstein, J. H., Rao, P. S. C., & Jawitz, J. W. (2017). Emergent archetype patterns of coupled hydrologic and biogeochemical responses in catchments. *Geophysical Research Letters*, 44(9), 4143-4151.
- Musolff, A., Grau, T., Weber, M., Ebeling, P., Samaniego-Eguiguren, L., & Kumar, R. (2020). *WQADB: water quality and quantity data base Germany*. Retrieved from: <http://www.ufz.de/record/dmp/archive/7754>
- Musolff, A., Schmidt, C., Selle, B., & Fleckenstein, J. H. (2015). Catchment controls on solute export. *Advances in Water Resources*, 86, 133-146.
- Musolff, A., Selle, B., Buttner, O., Opitz, M., & Tittel, J. (2017). Unexpected release of phosphate and organic carbon to streams linked to declining nitrogen depositions. *Glob Chang Biol*, 23(5), 1891-1901. <https://www.ncbi.nlm.nih.gov/pubmed/27614066>
- Oelsner, G. P., Sprague, L. A., Murphy, J. C., Zuellig, R. E., Johnson, H. M., Ryberg, K. R., et al. (2017). *Water-Quality Trends in the Nation's Rivers and Streams, 1972–2012—Data Preparation, Statistical Methods, and Trend Results*. Retrieved from
- Oldham, C. E., Farrow, D. E., & Peiffer, S. (2013). A generalized Damköhler number for classifying material processing in hydrological systems. *Hydrol. Earth Syst. Sci.*, 17(3), 1133-1148. <https://www.hydrol-earth-syst-sci.net/17/1133/2013/>
- Onderka, M., Wrede, S., Rodný, M., Pfister, L., Hoffmann, L., & Krein, A. (2012). Hydrogeologic and landscape controls of dissolved inorganic nitrogen (DIN) and dissolved silica (DSi) fluxes in heterogeneous catchments. *Journal of Hydrology*, 450-451, 36-47.
- Ouedraogo, I., Defourny, P., & Vanclooster, M. (2019). Application of random forest regression and comparison of its performance to multiple linear regression in modeling groundwater nitrate concentration at the African continent scale. *Hydrogeology Journal*, 27(3), 1081-1098. <https://doi.org/10.1007/s10040-018-1900-5>
- Pascal, P. Y., Fleeger, J. W., Boschker, H. T. S., Mitwally, H. M., & Johnson, D. S. (2013). Response of the benthic food web to short- and long-term nutrient enrichment in saltmarsh mudflats. *Marine Ecology Progress Series*, 474, 27-41. <http://www.int-res.com/abstracts/meps/v474/p27-41/>
- Pflugmacher, D., Rabe, A., Peters, M., & Hostert, P. (2018). *Pan-European land cover map of 2015 based on Landsat and LUCAS data*. Retrieved from: <https://doi.org/10.1594/PANGAEA.896282>
- Pinay, G., Peiffer, S., De Dreuz, J.-R., Krause, S., Hannah, D. M., Fleckenstein, J. H., et al. (2015). Upscaling Nitrogen Removal Capacity from Local Hotspots to Low Stream Orders' Drainage Basins. *Ecosystems*, 18(6), 1101-1120. journal article. <https://doi.org/10.1007/s10021-015-9878-5>
- Rivett, M. O., Buss, S. R., Morgan, P., Smith, J. W. N., & Bemment, C. D. (2008). Nitrate attenuation in groundwater: A review of biogeochemical controlling processes. *Water Research*, 42(16), 4215-4232. <http://www.sciencedirect.com/science/article/pii/S0043135408002984>
- Rodriguez-Galiano, V., Mendes, M. P., Garcia-Soldado, M. J., Chica-Olmo, M., & Ribeiro, L. (2014). Predictive modeling of groundwater nitrate pollution using Random Forest and multisource variables related to intrinsic and specific vulnerability: A case study in an agricultural setting (Southern Spain). *Science of The Total Environment*, 476-477, 189-206. <http://www.sciencedirect.com/science/article/pii/S0048969714000102>
- Rose, L. A., Karwan, D. L., & Godsey, S. E. (2018). Concentration–discharge relationships describe solute and sediment mobilization, reaction, and transport at event and longer timescales. *Hydrological Processes*, 32(18), 2829-2844. [http://https://doi.org/10.1002/hyp.13235](https://doi.org/10.1002/hyp.13235)
- Rozemeijer, J. C., van der Velde, Y., van Geer, F. C., Bierkens, M. F. P., & Broers, H. P. (2010). Direct measurements of the tile drain and groundwater flow route contributions to surface water contamination: From field-scale concentration patterns in groundwater to catchment-scale surface water quality. *Environmental Pollution*, 158(12), 3571-3579. <http://www.sciencedirect.com/science/article/pii/S0269749110003672>
- Sabater, S., Butturini, A., Clement, J.-C., Burt, T., Dowrick, D., Hefting, M., et al. (2003). Nitrogen Removal by Riparian Buffers along a European Climatic Gradient: Patterns and Factors of Variation. *Ecosystems*, 6(1), 0020-0030. journal article. <https://doi.org/10.1007/s10021-002-0183-8>
- Samaniego, L., Kumar, R., & Attinger, S. (2010). Multiscale parameter regionalization of a grid-based hydrologic model at the mesoscale. *Water Resources Research*, 46(5). [http://https://doi.org/10.1029/2008WR007327](https://doi.org/10.1029/2008WR007327)

- Schmidt, L., Heße, F., Attinger, S., & Kumar, R. (2020). Challenges in applying machine learning models for hydrological inference: A case study for flooding events across Germany. *Water Resources Research*, n/a(n/a), e2019WR025924. <https://agupubs.onlinelibrary.wiley.com/doi/abs/10.1029/2019WR025924>
- Schoumans, O. F., Bouraoui, F., Kabbe, C., Oenema, O., & van Dijk, K. C. (2015). Phosphorus management in Europe in a changing world. *Ambio*, 44(2), 180-192. <https://doi.org/10.1007/s13280-014-0613-9>
- Schoumans, O. F., Chardon, W. J., Bechmann, M. E., Gascuel-Oudou, C., Hofman, G., Kronvang, B., et al. (2014). Mitigation options to reduce phosphorus losses from the agricultural sector and improve surface water quality: a review. *Sci Total Environ*, 468-469, 1255-1266. <https://www.ncbi.nlm.nih.gov/pubmed/24060142>
- Seibert, J., Grabs, T., Köhler, S., Laudon, H., Winterdahl, M., & Bishop, K. (2009). Linking soil- and stream-water chemistry based on a Riparian Flow-Concentration Integration Model. *Hydrol. Earth Syst. Sci.*, 13(12), 2287-2297. <https://www.hydrol-earth-syst-sci.net/13/2287/2009/>
- Shangguan, W., Hengl, T., Mendes de Jesus, J., Yuan, H., & Dai, Y. (2017). Mapping the global depth to bedrock for land surface modeling. *Journal of Advances in Modeling Earth Systems*, 9(1), 65-88. <https://agupubs.onlinelibrary.wiley.com/doi/abs/10.1002/2016MS000686>
- Sharpley, A., Jarvie, H. P., Buda, A., May, L., Spears, B., & Kleinman, P. (2013). Phosphorus Legacy: Overcoming the Effects of Past Management Practices to Mitigate Future Water Quality Impairment. *Journal of Environmental Quality*, 42(5), 1308-1326. <https://access.onlinelibrary.wiley.com/doi/abs/10.2134/jeq2013.03.0098>
- Smith, V. H. (2003). Eutrophication of freshwater and coastal marine ecosystems a global problem. *Environmental Science and Pollution Research*, 10(2), 126-139. journal article. <https://doi.org/10.1065/espr2002.12.142>
- Smith, V. H., Tilman, G. D., & Nekola, J. C. (1999). Eutrophication: impacts of excess nutrient inputs on freshwater, marine, and terrestrial ecosystems. *Environmental Pollution*, 100(1), 179-196. <http://www.sciencedirect.com/science/article/pii/S0269749199000913>
- Taylor, P. G., & Townsend, A. R. (2010). Stoichiometric control of organic carbon–nitrate relationships from soils to the sea. *Nature*, 464, 1178. <https://doi.org/10.1038/nature08985>
- Tetzlaff, B., Kuhr, P., & Wendland, F. (2009). A new method for creating maps of artificially drained areas in large river basins based on aerial photographs and geodata. *Irrigation and Drainage*, 58(5), 569-585. <https://onlinelibrary.wiley.com/doi/abs/10.1002/ird.426>
- Thompson, S. E., Basu, N. B., Lascrain, J., Aubeneau, A., & Rao, P. S. C. (2011). Relative dominance of hydrologic versus biogeochemical factors on solute export across impact gradients. *Water Resources Research*, 47(10). <https://agupubs.onlinelibrary.wiley.com/doi/full/10.1029/2010WR009605>
- Tunaley, C., Tetzlaff, D., & Soulsby, C. (2017). Scaling effects of riparian peatlands on stable isotopes in runoff and DOC mobilisation. *Journal of Hydrology*, 549, 220-235. <http://www.sciencedirect.com/science/article/pii/S0022169417301956>
- Underwood, K. L., Rizzo, D. M., Schroth, A. W., & Dewoolkar, M. M. (2017). Evaluating Spatial Variability in Sediment and Phosphorus Concentration-Discharge Relationships Using Bayesian Inference and Self-Organizing Maps. *Water Resources Research*, 53(12), 10293-10316. <https://agupubs.onlinelibrary.wiley.com/doi/abs/10.1002/2017WR021353>
- Van der Velde, Y., Rooij, G. H. d., Rozemeijer, J. C., Geer, F. C. v., & Broers, H. P. (2010). Nitrate response of a lowland catchment: On the relation between stream concentration and travel time distribution dynamics. *Water Resources Research*, 46(11). <http://https://doi.org/10.1029/2010WR009105>
- Van Meter, K. J., & Basu, N. B. (2015). Catchment legacies and time lags: a parsimonious watershed model to predict the effects of legacy storage on nitrogen export. *PLoS One*, 10(5), e0125971. <https://www.ncbi.nlm.nih.gov/pubmed/25985290>
- Van Meter, K. J., & Basu, N. B. (2017). Time lags in watershed-scale nutrient transport: an exploration of dominant controls. *Environmental Research Letters*, 12(8), 084017. <http://dx.doi.org/10.1088/1748-9326/aa7bf4>
- Wallin, M. B., Weyhenmeyer, G. A., Bastviken, D., Chmiel, H. E., Peter, S., Sobek, S., & Klemetsson, L. (2015). Temporal control on concentration, character, and export of dissolved organic carbon in two hemiboreal headwater streams draining contrasting catchments. *Journal of Geophysical Research: Biogeosciences*, 120(5), 832-846. <https://agupubs.onlinelibrary.wiley.com/doi/abs/10.1002/2014JG002814>
- Wang, L., Stuart, M. E., Lewis, M. A., Ward, R. S., Skirvin, D., Naden, P. S., et al. (2016). The changing trend in nitrate concentrations in major aquifers due to historical nitrate loading from agricultural land across England and Wales from 1925 to 2150. *Sci Total Environ*, 542(Pt A), 694-705. <https://www.ncbi.nlm.nih.gov/pubmed/26546765>

- Wen, H., Perdrial, J., Abbott, B. W., Bernal, S., Dupas, R., Godsey, S. E., et al. (2020). Temperature controls production but hydrology regulates export of dissolved organic carbon at the catchment scale. *Hydrol. Earth Syst. Sci.*, 24(2), 945-966. <https://www.hydrol-earth-syst-sci.net/24/945/2020/>
- Wendland, F., Blum, A., Coetsiers, M., Gorova, R., Griffioen, J., Grima, J., et al. (2008). European aquifer typology: a practical framework for an overview of major groundwater composition at European scale. *Environmental Geology*, 55(1), 77-85. <https://doi.org/10.1007/s00254-007-0966-5>
- Werner, B. J., Musolff, A., Lechtenfeld, O. J., de Rooij, G. H., Oosterwoud, M. R., & Fleckenstein, J. H. (2019). High-frequency measurements explain quantity and quality of dissolved organic carbon mobilization in a headwater catchment. *Biogeosciences*, 16(22), 4497-4516. <https://www.biogeosciences.net/16/4497/2019/>
- Westphal, K., Graeber, D., Musolff, A., Fang, Y., Jawitz, J. W., & Borchardt, D. (2019). Multi-decadal trajectories of phosphorus loading, export, and instream retention along a catchment gradient. *Science of The Total Environment*, 667, 769-779. <http://www.sciencedirect.com/science/article/pii/S0048969719309404>
- Wilde, S., Hansen, C., & Bergmann, A. (2017). Nachlassender Nitratabbau im Grundwasser und deren Folgen – abgestufte modellgestützte Bewertungsansätze (engl. Decreasing denitrification capacity in aquifers: scaled model-based evaluation). *Grundwasser*, 22(4), 293-308. <https://doi.org/10.1007/s00767-017-0373-0>
- Winterdahl, M., Erlandsson, M., Futter, M. N., Weyhenmeyer, G. A., & Bishop, K. (2014). Intra-annual variability of organic carbon concentrations in running waters: Drivers along a climatic gradient. *Global Biogeochemical Cycles*, 28(4), 451-464. <https://agupubs.onlinelibrary.wiley.com/doi/abs/10.1002/2013GB004770>
- Winterdahl, M., Futter, M., Köhler, S., Laudon, H., Seibert, J., & Bishop, K. (2011). Riparian soil temperature modification of the relationship between flow and dissolved organic carbon concentration in a boreal stream. *Water Resources Research*, 47(8). <https://agupubs.onlinelibrary.wiley.com/doi/abs/10.1029/2010WR010235>
- Withers, P. J. A., & Jarvie, H. P. (2008). Delivery and cycling of phosphorus in rivers: A review. *Science of The Total Environment*, 400(1), 379-395. <http://www.sciencedirect.com/science/article/pii/S0048969708008139>
- Withers, P. J. A., May, L., Jarvie, H. P., Jordan, P., Doody, D., Foy, R. H., et al. (2012). Nutrient emissions to water from septic tank systems in rural catchments: Uncertainties and implications for policy. *Environmental Science & Policy*, 24, 71-82. <http://www.sciencedirect.com/science/article/pii/S1462901112001293>
- WMO. (2008). *Manual on Low-flow Estimation and Prediction*. Retrieved from http://library.wmo.int/pmb_ged/wmo_1029_en.pdf
- Wold, S., Sjöström, M., & Eriksson, L. (2001). PLS-regression: a basic tool of chemometrics. *Chemometrics and Intelligent Laboratory Systems*, 58(2), 109-130. <http://www.sciencedirect.com/science/article/pii/S0169743901001551>
- Zarnetske, J. P., Bouda, M., Abbott, B. W., Saiers, J., & Raymond, P. A. (2018). Generality of Hydrologic Transport Limitation of Watershed Organic Carbon Flux Across Ecoregions of the United States. *Geophysical Research Letters*, 45(21), 11,702-711,711. <https://agupubs.onlinelibrary.wiley.com/doi/abs/10.1029/2018GL080005>
- Zhi, W., Li, L., Dong, W., Brown, W., Kaye, J., Steefel, C., & Williams, K. H. (2019). Distinct Source Water Chemistry Shapes Contrasting Concentration-Discharge Patterns. *Water Resources Research*, 55(5), 4233-4251. <https://agupubs.onlinelibrary.wiley.com/doi/abs/10.1029/2018WR024257>
- Zimmer, M. A., Pellerin, B., Burns, D. A., & Petrochenkov, G. (2019). Temporal variability in nitrate-discharge relationships in large rivers as revealed by high-frequency data. *Water Resources Research*, 0(0). <https://agupubs.onlinelibrary.wiley.com/doi/abs/10.1029/2018WR023478>
- Zink, M., Kumar, R., Cuntz, M., & Samaniego, L. (2017). A high-resolution dataset of water fluxes and states for Germany accounting for parametric uncertainty. *Hydrology and Earth System Sciences*, 21(3), 1769-1790.